2013

Generation and Characterization of Peptide Fusion Proteins

Brianna L. Probasco
Rowan University

GENERATION AND CHARACTERIZATION OF PEPTIDE FUSION PROTEINS

Brianna L Probasco, B.A.

A Dissertation submitted to the Graduate School of Biomedical Sciences, previously of the University of Medicine and Dentistry of New Jersey, now a part of Rowan University, in partial fulfillment of the requirements for the M.S. Degree.

Stratford, New Jersey 08084

December 2013

Table of Contents

Acknowledgements

First and foremost, I would like to sincerely thank each member, past and present, of Humigen LLC for guiding this work with their advice and technical expertise. I would especially like to thank Dr. Grant Gallagher, Dr. Raymond Yu, and Dr. Anibal Valentín-Acevedo for their mentorship and guidance. I would also like to thank my thesis committee: Dr. Grant Gallagher, Dr. Raymond Yu, Dr. Kathryn Iacono, and Dr. Venkat Venkataraman, as well as, Dr. Diane Worrad for all of her help along the way.

I am also grateful for the love and support of my parents, Marc Probasco and Diane Sullivan. And a special thanks to Dr. John Taylor of Rutgers University and Dr. Kusum Punjabi of Robert Wood Johnson University Hospital for encouragement to pursue my studies further.

Finally, I would like to express my appreciation to Dr. Eli Morechai, CEO of Medical Diagnostic Laboratories for providing a well-equipped state-of-the-are facility and the funding which enabled me to perform this research.

Abstract

Pathogenic Th17 cells drive progression of many autoimmune diseases. Th17 cells develop from naïve T cells in the immune system after antigen-driven stimulation in a specific cytokine environment. Normally, T cells act to fight off infection, but when not properly controlled, they can cause disease. The cytokine interleukin-23 (IL-23) plays an essential role in the expansion of pathogenic Th17 cells. IL-23 is a heterodimeric protein, composed of a p19 alpha chain and a p40 beta chain. The p40 is also part of IL-12 and binds to the IL-12 receptor beta 1 (IL-12Rβ1) subunit. Thus, it follows that the IL-23 receptor is comprised of the IL-12Rβ1 and IL-23 receptor alpha (IL23Rα) subunits. New research in therapeutics for autoimmune disease is attempting to inhibit IL-23 from binding to its receptor. Our laboratory previously screened a peptide library through display technologies for peptides that bound to the IL-23Rα. Peptides #7 and #2 were identified as having the strongest inhibitory activity on the IL-23 signaling pathway. However, peptides are small, leading them to be cleared from a biological system in a manner of minutes; therefore, the present project created fusion proteins of these peptides with mouse IgG2a-Fc. They were then expressed in mammalian cells, secreted and purified from medium. Peptide #2-Fc and its unmodified counterpart, Peptide #2, were tested and compared using cell-free and cell-based systems to ensure minimal loss of inhibitory activity upon fusion. This work generated a Peptide #2-Fc fusion protein with the capability to bind the IL23Rα chain and

thus block IL-23 binding and inhibit subsequent signaling, as well an increased serum half-life over the original Peptide #2.

1. Introduction

In 2005, the National Institute of Health (NIH) estimated that 5-8% of the population in the United States (15-24 million people) was affected by an autoimmune condition (NIH report, 2005). In total, there are over eighty different known classified autoimmune diseases with the most common being: type-1 diabetes, rheumatoid arthritis, systemic lupus erythematosus, inflammatory bowel disease (IBD) and asthma. With the progression of these chronic, life-long diseases, many patients eventually require surgery, increased nursing care and more frequent and longer hospitalizations. Therefore, treatments to alleviate disease symptoms are highly needed.

In recent years, some autoimmune diseases have been shown to have a similar disease mechanism driven by Th17 cells. Th17 cells, a subset of CD4+ effector cells, are characterized by the production of pro-inflammatory cytokines including interleukins (IL)-17, 22, and 26.

1.1 Th17 cells in Inflammatory autoimmune diseases

Th17 cells drive many autoimmune diseases including but not limited to inflammatory bowel diseases (IBD), psoriasis, and multiple sclerosis (MS). These diseases are chronic and debilitating, and combined are among the top ten leading causes of death for women younger than 64 (Walsh & Rau, 2000). IBD patients also face a high likelihood of needing surgery, which has driven their overall healthcare cost to $1.7 billion dollars per year (CDC, 2011). Other current non-surgical treatments for disease focus on the management

of symptoms with broad spectrum, non-specific antibiotics and steroids. There are no treatments that directly influence the cause of symptoms, Th17 cells or the IL-23/Th17 axis.

1.2 Th17 cell differentiation

Th17 cells are named for and characterized by their interleukin (IL)-17 and other pro-inflammatory cytokines including IL- 22 and 26 (Harrington et al., 2005). IL-17 production by Th17 cells is conferred after expression of the transcription factor retinoic acid-related orphan receptor (ROR) γT (Ivanov et al., 2006). As such RORγT is the distinguishing transcription factor for Th17 cells (figure 1). RORγT is induced in naive CD4+ T cells through the binding of IL-6, IL-1β, and TGFβ to the T cell antigen receptors (TCR). This signaling also initiates an autocrine positive feedback loop of IL-21 production. IL-21 is required for expression of the IL-23 receptor (IL-23R) on the cell surface Th17 cells (Zhou et al., 2007). IL-23 signaling through the receptor enhances IL-17 production, solidifies the Th17 cell lineage, and promotes expansion of the subset. This importance has made IL-23 signaling an appealing therapeutic target.

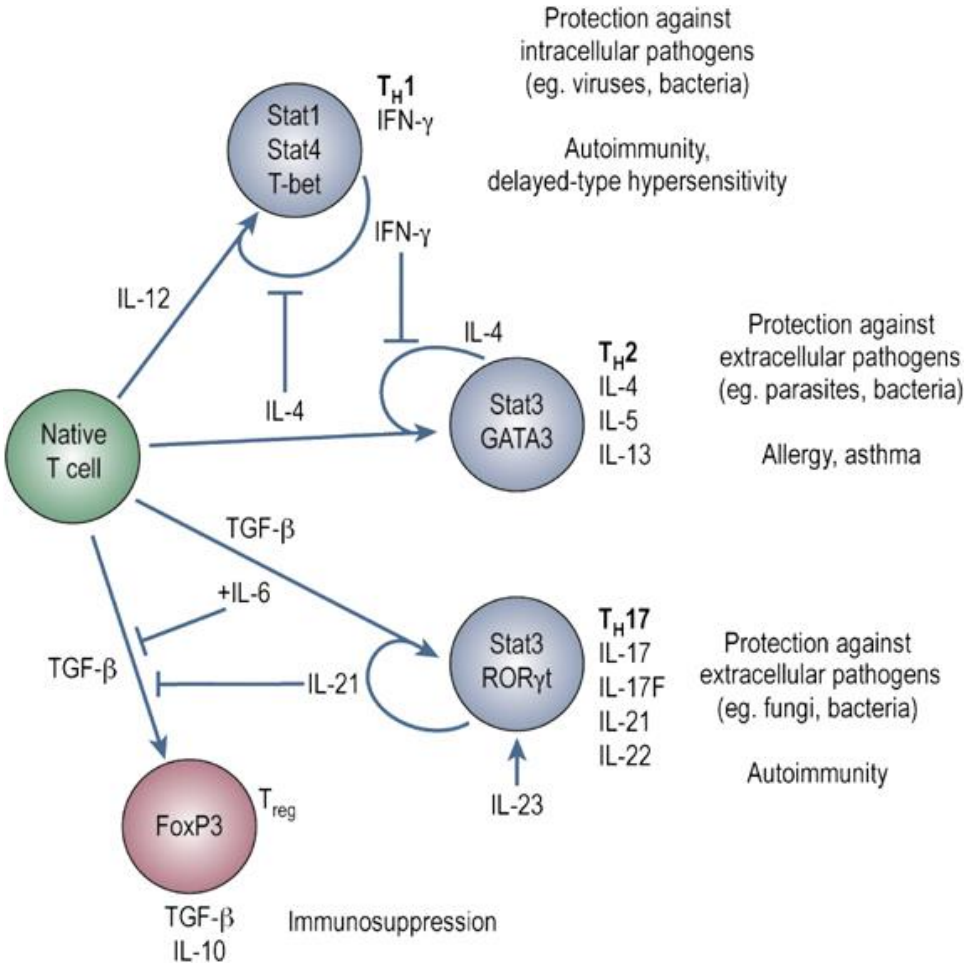

Figure 1. Differentiation of T Helper Cells. Image from Deenick & Tangye, 2007.

1.3 Interleukin-23 cytokine, receptor, and signaling

The p19 molecule was discovered in 2000 during a database sequence screening for IL-6 cytokine family members (Oppmann et al., 2000). The study proceeded to investigate the properties of this molecule and thus define a new cytokine, IL-23. The p19 subunit forms a disulfide bond with the IL-12 common p40 subunit to create the biologically active heterodimeric IL-23. Activated macrophages and dendritic cells (DCs) are the main producers of IL-23. Differential studies confirmed the extent of IL-23 verses IL-12 activity in disease status through the expression levels of p19 in various disease models. This led to the further investigation of IL-23 as a major prognostic indicator of disease. Maddur et al. demonstrated a clear relationship of the IL-23/Th17 axis to the pathogenesis of RA, systemic lupus erythematosus, multiple sclerosis, psoriasis, IBD, and asthma in a review of current data (2012).

The IL-23 receptor (IL23R) consists of the IL-12 receptor subunit, IL-12Rβ1, and a unique subunit, IL-23Rα (Parham et al., 2002). As anticipated the p19 subunit binds to the IL-23Rα receptor chain, while p40 binds to its IL-12Rβ1 as seen in the IL-12 system (figure 2). A naturally occurring, soluble IL23R occurs through the translation of IL-23R mRNA with exon 9 omitted (Yu & Gallagher, 2010). This form, "Δ9," contains the entire external domain and is predicted to act as part of a regulatory mechanism to suppress Th17 cell proliferation and production of IL-17. The IL-23Rα signals thru Janus kinase 2 (JAK2), which binds to the receptor chain's intracellular domain, to phosphorylate STAT3 (Parham et al., 2002). Phosphorylated STAT3 then

dimerizes, enters the nucleus, and promotes transcription of IL-17A, IL-17F, IL-22, and debatably IFNγ.

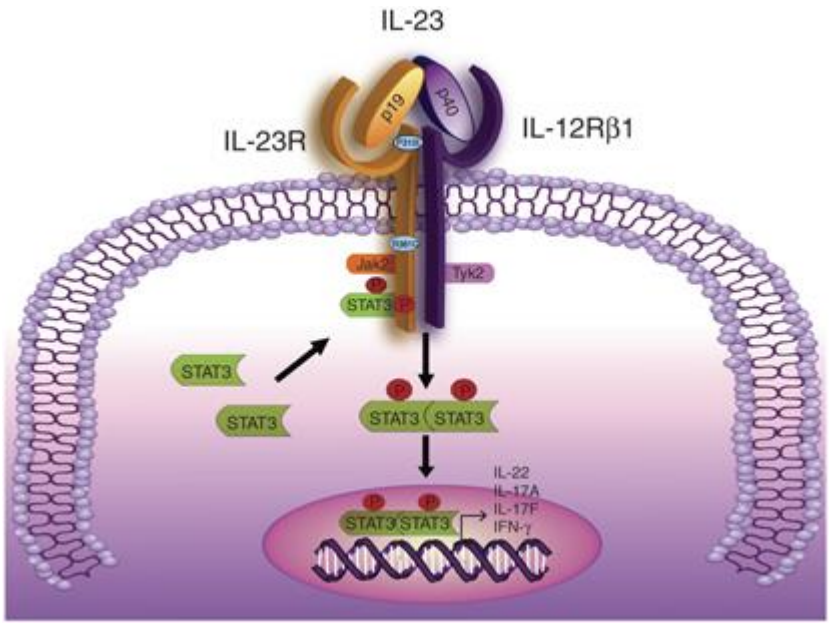

Figure 2. Interleukin 23 Binding & Receptor Signaling. Image from Di Cesare, Di Meglio, & Nestle, 2009.

1.4 Therapeutic peptides and the use of Fc fusion delivery

Our laboratory has been working to identify potential peptides that bind to the IL23R and block subsequent IL-23 signaling. Using display technologies, a series of inhibitory peptides were elucidated. Among them, peptides #2 and #7 showed similar inhibitory activity, while peptide #2 was also detected more frequently. Since only the amino acid sequence and not the structure of the IL-23R has been determined, when work was begun to create an IL-23R antagonist, screening large peptide libraries in phage display for potential binding was determined to be the most efficient approach (Gallagher et al., *20,130,029,907*). The first round of experimentation screened a library of 10^{11} random peptides using M13 phage to display peptides to the extracellular domain of human IL-23R fused with Fc region of human IgG1 (purchased from R&D). A second was conducted using Δ9, the soluble form of the IL23R with intact binding region (Yu & Gallagher, 2010), in place of the human IL-23R. While not a good therapeutic agent itself because it binds to the IL-23 cytokine with equivalent affinity as the full receptor, Δ9 is a good screening agent because it binds specifically to the p19 chain of IL-23. Non-specifically binding phages were eliminated through a negative selection step during each selection round. Selection pressure was increased through incrementally decreasing the amount of target. After three rounds of selection, a series of peptides containing a **WXXYW** motif, in which X could be any amino acid, was observed. A cell-free competitive ELISA confirmed that these peptides bound to IL-23R in a specific manner and allowed for comparison among the

peptides for their inhibitory activity. Those peptides with the greatest inhibitory activity in the cell-free assay were also assessed via a cell-based luciferase assay. This assay was developed to monitor the phosphorylation of STAT3, the downstream effect of IL-23 binding to its receptor as shown earlier. This same effect was also observed through western blot. In this manner, peptide #23, with the amino acid sequence of **AMTWEDEWLYGR,** was determined to have the best inhibitory activity on the IL-23R pathway.

Sequence manipulation experiments were then completed to establish optimal sequence length and determine critical amino acids of the motif. Substitution of either or both tryptophan residues resulted in abrogation of the inhibitory effect of the peptide. Other amino acid substitutions were made in and around the core motif, as well as, truncations and additions from nine to eighteen amino acids were used to test for the optimal length of the peptides. Ultimately, peptide #23.12 with the sequence: **AMTWQDYWLYGR**, was determined to have the strongest inhibitory activity to the IL-23R pathway.

Although peptide #23.12 worked well, the data were relative to the initial library of only 10^{11} peptides out of the possible 20^{12} peptides for the twelve amino acid length peptide. In order to increase confidence of having a peptide with the highest inhibitory activity, a new peptide library was generated with the **WXXYW** core motif fixed (Gallagher et al., *20,130,172,272*). This library was screened using ribosomal display with the same positive and negative selection agents as previously employed. Ribosomal display allowed for the joining of the phenotypic peptides to their

genotypic mRNA, which underwent RT-PCR instead of relying on the phage system. The peptides identified through this method were then compared with the peptide #23.12 for inhibitory activity. Combination of both display techniques identified the promising IL-23R antagonists, peptides #2 and #7, with the amino acid sequence shown in Table 1.

However, peptides are not good therapeutic agents. If given orally, they are metabolized in the gastrointestinal tract, or if administered by subcutaneous injection, their small size results in high rates of kidney clearance and serum protease degradation. Therefore, it is necessary to increase the peptide's serum half-life. To achieve this, peptides can be fused to the Fc portion of an immunoglobulin (Ig) as depicted in Figure 3. Enbrel (etanercept), a fusion protein in which, the TNF receptor-binding region was fused to the Fc region of IgG1 (Peppel et al., 1991), has successfully accomplished not only in theory but as a marketable drug therapy for over a decade already. This approach was not feasible for the IL23R because adding an IL-23 like peptide would mostly induce signaling, no longer incurring any therapeutic value.

However, combining Fc fusion protein technology with the earlier mentioned IL23R antagonist peptides would be a viable option. Using this approach, well-tested Peptides #2 and #7 become possible therapies for many of the aforementioned autoimmune diseases, because the larger Fc portion of the fusion proteins will increase their serum half-life and inhibit kidney clearance. This study focuses on fusion of Peptides #2 and #7 to

mouse IgG2a Fc and consequent characterization of their fusion proteins as IL23R antagonists.

Table 1. Peptide Amino Acid Sequences.

Polypeptide Number	Amino Acid Sequence
#7	MKTWVDYWLETQ
#7Mutant	MKTAVDYALETQ
#2	KMTWVDYWLKNC
#2Mutant	KMTAVDYALKNC

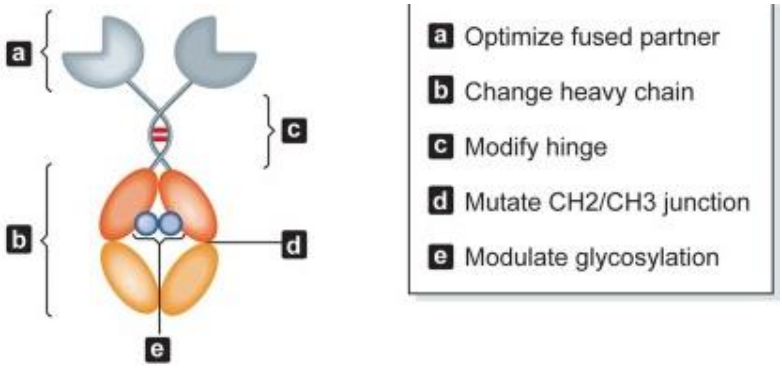

Figure 3. Structure of IgG Fc-fusion protein. Image from Czajkowsky, et al., 2012.

2. Rationale

The goal of this study is to create and characterize a peptide Fc fusion protein to advance the peptide's competence as a possible therapy against the IL-23 receptor. Peptides #2 and #7 have previously been proven efficacious in antagonizing the IL-23 receptor and inhibiting IL-23 binding, as well as downstream effects. As described earlier, IL-23 caused intracellular signaling within Th17 cells that incite a pathogenic role in many autoimmune diseases, including but not limited to IBD, psoriasis, and MS.

Extensive work in this laboratory has been completed in the selection of these peptides based on their ability to bind directly to the IL-23Rα chain specifically. Thus, these peptides inhibit IL-23 signaling and not IL-12 signaling. However, it is widely accepted that peptides are quickly degraded in vivo by proteases and have a high clearance rate by the kidneys. Using these peptides in the generation of an Fc fusion protein will effectively address these issues.

In addition, the Peptide #2-Fc fusion protein was tested in all the same assays that the original peptides were run through in order to confirm that Peptide #2 retained biological activity in this modification.

3. Materials and Methods

3.1 Fc-Fusion Plasmid Generation

2µg of the pFUSE-mIgG2Aa1-Fc2 plasmid (InvivoGen, pfc2-mg2ae1) was digested with 1µL NcoI and 1µL BglII in a total reaction volume of 30µL 1x NEBuffer 3 (New England BioLabs, R0193, R0144, & B7003S). The reaction was incubated in a 37°C heat block for 2 hours. Products were then purified on a 1% (w/v) agarose gel in Tris/Borate/EDTA (TBE) run for 35 minutes at 100 volts. The 4212bp band was visualized with ethidium bromide by UV light and extracted with QIAquick Gel Extraction Kit (QIAGEN, 28704). DNA was resuspended in 30µL of nuclease-free water, and concentration was measured on NanoDrop ND-1000 Spectrophotometer (Thermo Scientific).

Oligomers encoding the corresponding peptide sequences were designed and ordered from Integrated DNA Technologies (IDT) as described in Table 2. Extra nucleotides were added to bind to the sticky ends of the plasmid vector. 45µL of each forward and reverse primers at 100µM were annealed in 10µL 1x TE Buffer in 100°C heat block for five minutes and allowed to cool to room temperature in heat block. 2µL of each annealed oligomers were then ligated into 2.5µL (50ng)of the mIgG2Aa1-Fc2 plasmid in 1x DNA ligation buffer with 1µLT4 DNA ligase in 10µL T4 DNA ligation buffer (New England BioLabs, 04898117001) at room temperature for ten minutes (figure 4).

The ligation mixture was transformed into chemically competent TOP10 E. coli cells (Invitrogen) through heat shock. They were incubated on ice for 30 minutes then placed in a 42°C water bath for one minute, and returned to the ice for an additional two minutes. Cells were then recovered in S.O.C. bacterial growth medium for one hour in 37°C shaker, spun down and grown overnight on zeocin selective agar plates. Individual colonies were selected and cultured in 3mL zeocin selective Luria broth. The plasmid DNA was extracted using QIAprep Spin Miniprep Kit (QIAGEN, 27106).

1μg of plasmid DNA was digested with 1μL high fidelity HindIII and 1μL XhoI restriction enzymes in 1x NEBuffer 4 (New England BioLabs, R3104, R0146, & B7004S) at 37°C for 90 minutes. The digestion products were run on a 1.5% (w/v) agarose gel in TBE for 45 minutes at 100 volts. Bands were visualized using UV light box and ethidium bromide staining. Fragment sizes were established using Hyperladder IV (Bioline). The selected expression plasmids were validated by DNA sequencing. 500ng plasmid DNA was mixed with 5μM Fc forward primer and was sent to Genwiz, Inc.

Table 2: Primer Sequences Encoding Corresponding Peptides.

Peptide Number	Direction	Oligonucleotide Sequence
#7	F	C ATG GTT ATG AAG ACC TGG GTG GAC TAC TGG CTG GAG ACC CAG A
	R	GA TCT CTG GGT CTC CAG CCA GTA GTC CAC CCA GGT CTT CAT AAC
#7Mutant	F	C ATG GTT ATG AAG ACC GCC GTG GAC TAC GCC CTG GAG ACC CAG A
	R	GA TCT CTG GGT CTC CAG GGC GTA GTC CAC GGC GGT CTT CAT AAC
#2	F	C ATG GTT AAG ATG ACC TGG GTG GAC TAC TGG CTG AAG AAC TGC A
	R	GA TCT GCA GTT CTT CAG CCA GTA GTC CAC CCA GGT CAT CTT AAC
#2Mutant	F	C ATG GTT AAG ATG ACC GCC GTG GAC TAC GCC CTG AAG AAC TGC A
	R	GA TCT GCA GTT CTT CAG GGC GTA GTC CAC GGC GGT CAT CTT AAC

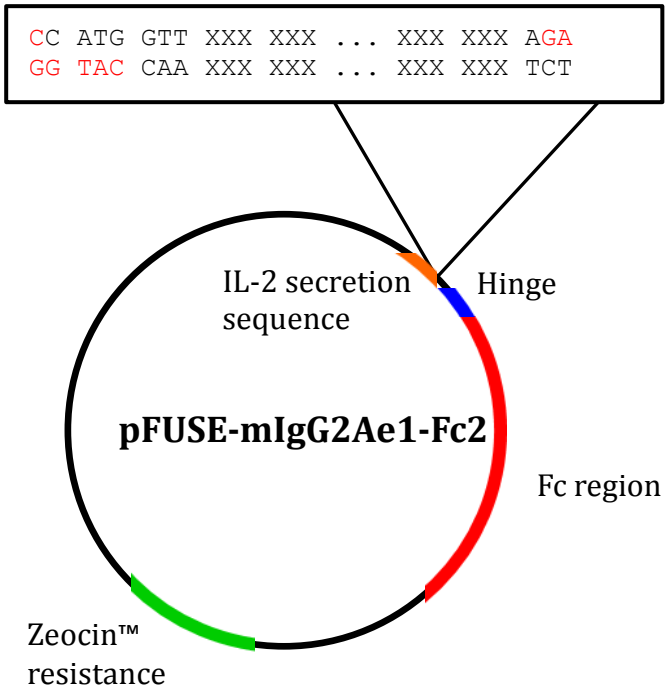

Figure 4. Plasmid Vector with Peptide Coding Sequence. Mouse IgG2a-Fc plasmid vector with important features highlighted. Blow-up shows cut plasmid nucleotides in red and peptide insertion sequence in black with sticky ends.

3.2 Cell Culture

The CHO-K1 (CCL-61) and 293T (CRL-3216) cells lines were purchased from American Tissue Culture Collection (ATCC; Rockville, MD). Both cell lines were maintained as described by ATCC. CHO-K1 cells were maintained in Ham's F-12K (Kaighn's) medium (Gibco, 21127-022) with 10% heat inactivated fetal bovine serum (Gibco, 10082-147). HEK239T cells were maintained in Dulbecco's Modified Eagle's Medium (DMEM; Sigma, D5796) with 10% heat inactivated fetal bovine serum (Gibco, 10082-147). Both cell lines were grown in 100mm culture plates to 70-90% confluence over four days then passaged by trypsinization using TrypLE™ Express (Gibco, 12604-013). Cells were plated at $2x10^5$ cells/well in 6-well plates or split 1:2.5 from 60.1cm^2 into 147.8cm^2 plates 24 hours prior to transfection.

Stable cells lines for protein expression were created from CHO-K1 cells. Cells were maintained in Ham's F-12K (Kaighn's) medium (Gibco, 21127-022) with 10% heat inactivated fetal bovine serum (Gibco, 10082-147) and 250µg/mL Zeocin™ (InvivoGen, ant-zn-1). Optimal Zeocin™ level was determined by two kill curve experiments. CHO-K1 cells were plated $2x10^5$ cells/well in 6-well plates 24 hours prior to first treatment. Cells were treated with Zeocin™ at 500µg/mL, 250µg/mL, 125µg/mL, 62.5µg/mL, 31.25µg/mL, and 0µg/mL every two to three days with medium change for two weeks. The ideal dose was considered to kill 90% of cells after seven to nine days and 100% of cells by two weeks.

3.2.1 Transfection Optimization

CHO-K1 cells were seeded at a density of $3x10^5$ and $4x10^5$ cells per well of a 6-well plates. 24 hours later, the $3x10^5$ cells per well density was 80% confluent and thus chosen for transfection. Cell medium was vacuumed off and replaced with fresh culture medium. 6:1, 3:1, and 1.5:1 ratios of FuGene 6 (Promega, E2691) lipid transfection reagent to 2µg GFP plasmid DNA (Lonza) were tested for GFP expression at 24 and 48 hours. FuGene6 was added to 200µL OPTI-MEM (Gibco, 31985) and incubated at room temperature for five minutes. DNA addition was followed by fifteen minutes incubation before adding to cells. Control cells were treated with 6µL FuGene6 in OPTI-MEM without DNA. Transfection efficiencies were assessed by flow cytometry (FACSCalibur, BD Biosciences) and analyzed using FlowJo software (figure5). The 6:1 ratio of FuGene6 to DNA was revealed to be too toxic with only approximately 60% of cells still alive at the 24 hour collection time point. Thus, the 3:1 ratio of FuGene6 to DNA collected at 48 hours was used for subsequent transfections with all Fc-fusion plasmids.

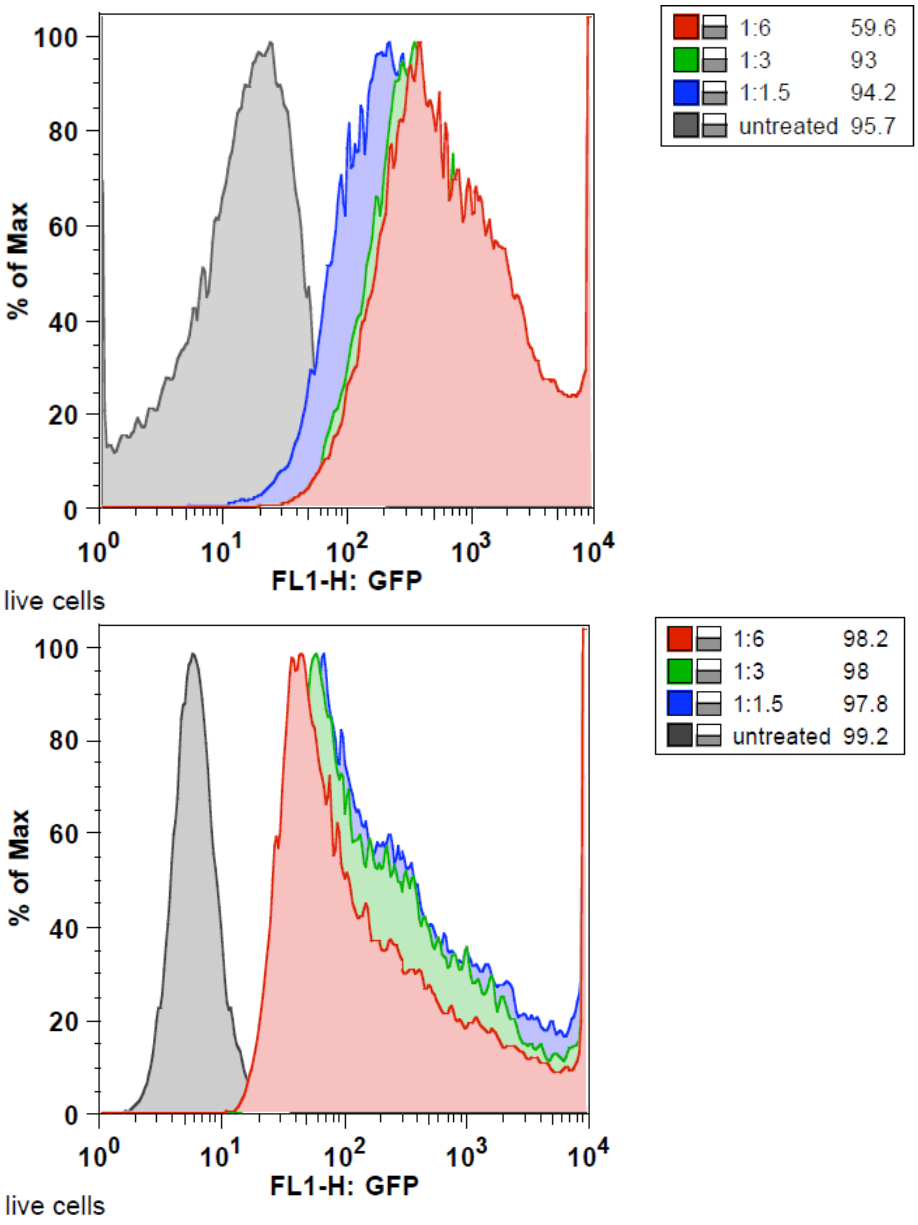

Figure 5. Transfection Efficiency of FuGene6 in CHO-K1 Cells. Green fluorescence protein transfected into Cho-K1 cells and harvested at 24 and 48 hours. Different ratios of FuGene6 to DNA were assessed for optimal expression with the lowest toxicity to cells.

3.3 Western Blotting

Cells and supernatants were collected 48 hours post transfection for protein analysis. Cells were either harvested by trysinization with TrypLE™ Express (Gibco) and pelleted and washed with 1x PBS or lysed in wells with 200µL ProteoJET™ Mammalian Cell Lysis Reagent(Fermentas, K0301) with protease inhibitor cocktail (Sigma, P8340). Cells pellets were later lysed in 1x RIPA buffer with protease inhibitor and assessed for protein concentration using a Bradford assay. ProteoJET collected samples were centrifuged at 16,000g at 4°C for 10 minutes. Cell supernatants were centrifuged at 16,000g for five minutes to pellet any non-adherent cells, and then cell-free supernatants were collected in 1.5mL tubes. All samples were stored at -20°C until used.

30µg of protein as measured by Bradford assay or 20µL ProteoJET samples were added to 4X XT Sample Buffer supplemented with XT Reducing Agent (BioRad, 161-0791 & 161-0792). Samples were boiled at 100°C for five minutes, then run on 18 well, 4-12% Bis-Tris Criterion™ XT Precast Gels (BioRad, 345-0125) in 1x MES buffer for 45 minutes at 200 volts. Proteins were transferred to PVDF membranes using wet transfer method in 1x Tris, Glycine, SDS buffer for 1 hour at 100 volts. 5% (w/v) milk in TBS/Tween20 (TBST) was used to block non-specific binding to membranes at room temperature for 1 hour. A goat α-mouse IgG-Fc_γ antibody (Pierce, 31439) 1:1000 or β-actin (Sigma, A5441) 1:2000 in 2.5% (w/v) milk in TBST were used for protein detection overnight at 4°C. Membranes were then washed with TBST. Protein-antibody signals were detected by a donkey α-goat IgG

horseradish-peroxidase (HRP) conjugated antibody (Santa Cruz, sc-2020) at 1:2000 in 2.5% (w/v) milk in TBST for 1 hour at room temperature. Membranes were then washed with TBST. After five minutes in SuperSignal West Dura Chemiluminescent Substrate (Thermo Scientific, 34075), blots were developed in ImageQuant LAS 4000 (GE) with accompanied software.

3.4 In Vitro Binding Assay

To confirm that peptide-Fc fusion did not abrogate peptide's ability to bind the IL23Rα, cell medium containing fusion protein and later pure protein were immunoprecipitated with Δ9 (figure 7). In the initial experiment, 1mL of cell culture medium containing Peptide #2-Fc was mixed with pre-washed 10μL of settled Protein A Resin (GenScript, L00210) on rotator for 1 hour at room temperature. Cell culture mediums containing Fc and Peptide #2Mutant-Fc were also assessed alongside as controls. Samples were spun down, supernatant removed; then medium containing Δ9 was added. They were incubated on rotator at 4°C overnight. Resin bound complexes were spun down and washed with 1x PBS ten times. 25μL 4X XT Sample Buffer supplemented with XT Reducing Agent was added to each sample and boiled at 100°C for five minutes. Total volume was run on SDS-PAGE and followed subsequent procedure described in section 3.3. After membrane blocking, blot was incubated at 4°C overnight in 1:1000 biotin conjugated α-IL23Rα antibody. A 1:2000 dilution of HRP linked streptavidin was used to detect binding complex-antibody signal.

Repeated experiment with pure protein was performed with 5μg of each fusion protein diluted to 200μL in 1x PBS following the same procedure.

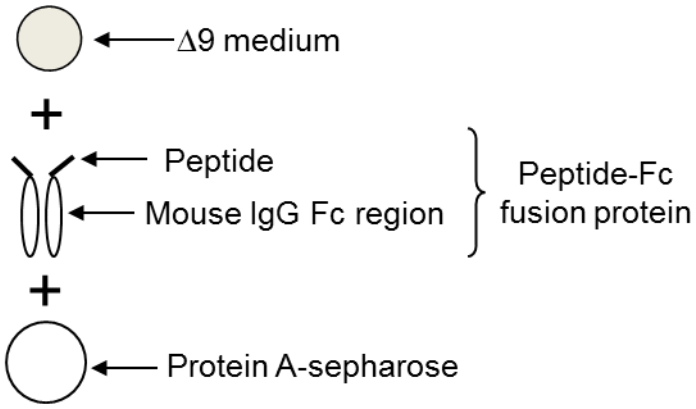

Figure 7. Immunoprecipitation with Δ9 Schematic.
Method to confirm binding activity of fusion protein to the IL-23 receptor.

3.5 ELISA

Mouse IgG2a ELISA was performed using the Ready-Set-Go ELISA kit (eBioscience, 88-50420-88) on supernatants from transient transfection and stables cells lines for productivity levels. The manufacturer's procedure was followed. Optical densities were measured by microplate reader (VERSAmax, Molecular Devices) and analyzed by SoftMax Pro software with a 4-parameter fit standard curve.

3.6 Protein Purification

Serum free Chemically Defined CHO (CD CHO) medium was used to replace maintenance medium in 150mm plates 24 hours post transfection or seeding of stable cells lines. CD CHO cell supernatant was collected 48 hours later, replaced and collected after another 48 hour time period. Cells were then discarded, and maintenance cells were used for subsequent collections. Supernatants were collected in 50mL conical tubes and centrifuged at 670g for ten minutes to remove any cellular debris. Samples were concentrated using 30K Amicon® Ultra Centrifugal Ultracel® Filters and stored at -20°C until both time points had been combined.

Pre-washed 1mL settled Protein A Resin or 500µL settled Ultra Protein A Resin (GenScript, L00400) was added to each collection of concentrated fusion protein containing supernatant and incubated overnight at 4°C. Samples were centrifuged at 670g at 4°C for ten minutes to gather beads for column packing. 5mL Centrifuge Columns (Pierce, 89897) were used for protein purification. Columns were washed with 50mL Protein A IgG

Binding Buffer (Pierce, 21001). Fusion proteins were eluted with 3mL IgG Elution Buffer (Pierce, 21004) twice and collected into 15mL conical tubes containing 600µL neutralizing UltraPure 1M Tris-HCl pH 8.0 (Invitrogen, 15568-025). Protein was concentrated again using 30K Amicon® Ultra Centrifugal Ultracel® Filters and concentrations of products measure on NanoDrop ND-1000 Spectrophotometer (Thermo Scientific).

3.7 Coomassie Blue

2µg of purified fusion protein, as calculated from A_{280} wavelength concentration, was loaded with 4X XT Sample Buffer containing XT Reducing Agent (BioRad, 161-0791 & 161-0792). Samples were run on 18 well, 4-12% Bis-Tris Criterion™ XT Precast Gels (BioRad, 345-0125) in 1x MES buffer for 45 minutes at 200 volts. Gel was stained with Bio-Safe Coomassie G-250 (BioRad, 161-0786) at room temperature for 1 hour, and then destained in double deionized water. Gel images were scanned in a GS-800 Calibrated Densitometer (BioRad) with Quantity One® software.

3.8 Competitive ELISA

This assay and conditions were previously determined by Dr. Raymond Yu (figure 6). IL-23R-Fc protein was coated on well of a 96-well plate with 100µL at 1µg/mL in 1x PBS overnight at 4°C. Plate was washed five times for 20 seconds each with wash buffer of 0.05% (v/v) Tween20 in 1x PBS, then blocked with 1x Assay Diluent (eBioscience, 88-7237-88) for 1 hour at room temperature. After washing once for ten seconds, all samples

and an IL-23 standard curve of: 250ng/mL, 62.5ng/mL, 15.625ng/mL, 7.8125ng/mL, 3.90625ng/mL, 0.9765625ng/mL, 0.244140625ng/mL, and 0ng/mL were added. Samples diluted in 1x Assay Diluent with IL-23 held at constant 15.625ng/mL were pre-mixed and added to wells of plate together and incubated at 4°C overnight. Plate was washed six times for one minute each, then incubated with a biotinylated anti-p40 detection antibody for 2 hours at room temperature. After washing again, avidin linked horseradish peroxidase detection enzyme was added and incubated for 1 hour at room temperature. Plates were washed five times for ten seconds each before adding TMB substrate reagent for a ten minute incubation at room temperature. 1M H_2SO_4 was used as a stop solution. The optical densities were read by VERSAmax microplate reader (Molecular Devices) and analyzed on SoftMax Pro software with a 4-parameter fit standard curve.

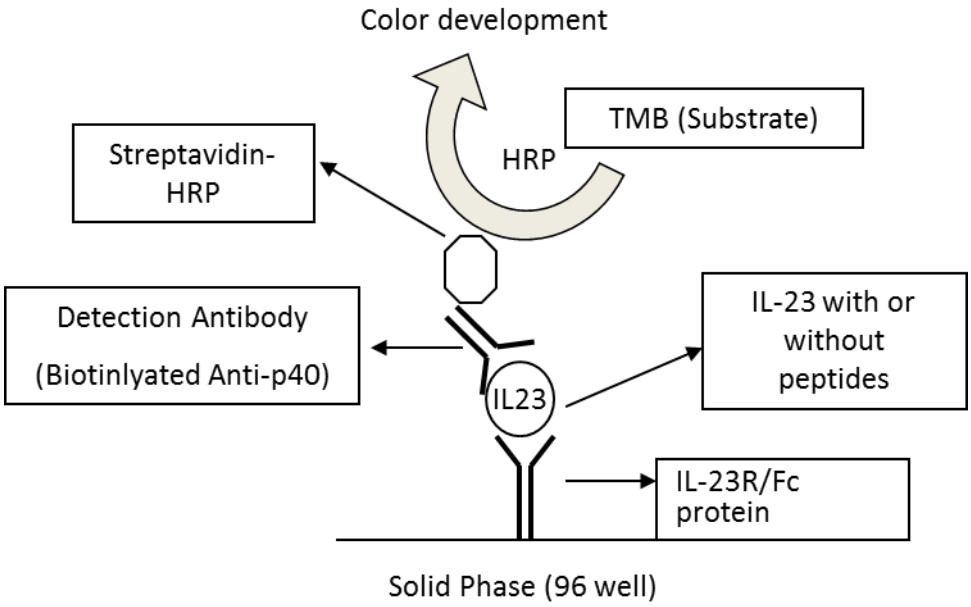

Figure 6. Explanation of IL-23 Competitive ELISA. When therapeutic peptide is present, it will bind to the IL-23 receptor and block cytokine binding. Therefore, the expected result of a good therapeutic agent is no signal or dampened signal as compared to an IL-23 standard curve.

3.9 STAT3-Luciferase Reporter Assay

STAT3-Luciferase reporter DB stable cells were previously generated by Dr. Raymond Yu, as well as the assay conditions described herein. DB reporter cells were seeded at $0.5x10^6$ cells per 100µL well in 96-well plates. Peptides (GenScript) resuspended at 5mM in DMSO or Fc-fusion protein samples in 1x PBS were added thirty minutes later. IL-23 cytokine was added in 2-fold dilution from 100ng/mL to 1.5625ng/mL for a standard curve and held constant in all peptide/protein treatment wells at 25ng/mL. Firefly luciferase activity upon phosphorylation of STAT3 was assessed using the Dual-Glo luciferase assay kit (Promega, E2940) four hours post stimulation. Luminescence was measured using a luminometer (LMax II 384, Molecular Devices).

3.10 Calculation of IC_{50} Values

The half maximal inhibitory concentrations (IC_{50}) of peptide #2 and Fc-fusion proteins were calculated from both the cell-free ELISA and the cell-based luciferase assays. Raw data were normalized via standard curves using elisaanalysis.com to give percentage IL-23 binding activity. These measures were used in computations versus the logarithm of treatment, peptide or Fc-fusion protein, concentration with GraphPad Prism software.

4. Experimental Results

4.1 Design and verification of peptide-Fc fusion plasmids

Eight sets of primers were designed for peptide #7 and #2, as well as mutant controls of both in which tryptophan residues were substituted for alanine. Additional nucleotides were added to assure peptide coding sequences would be in frame when annealed into the Fc plasmid vector. The fused vectors produced a plasmid of 4254bp total, while the mouse IgG2a Fc vector only was only 4212bp. This allowed for confirmation of peptide coding sequence fusion in plasmid through linearization by digest. Digestion products were then run on a 1.5% agarose gel (figure 8). Direct sequencing by GeneWiz verified peptide coding sequences were in the correct reading frame within the Fc plasmid.

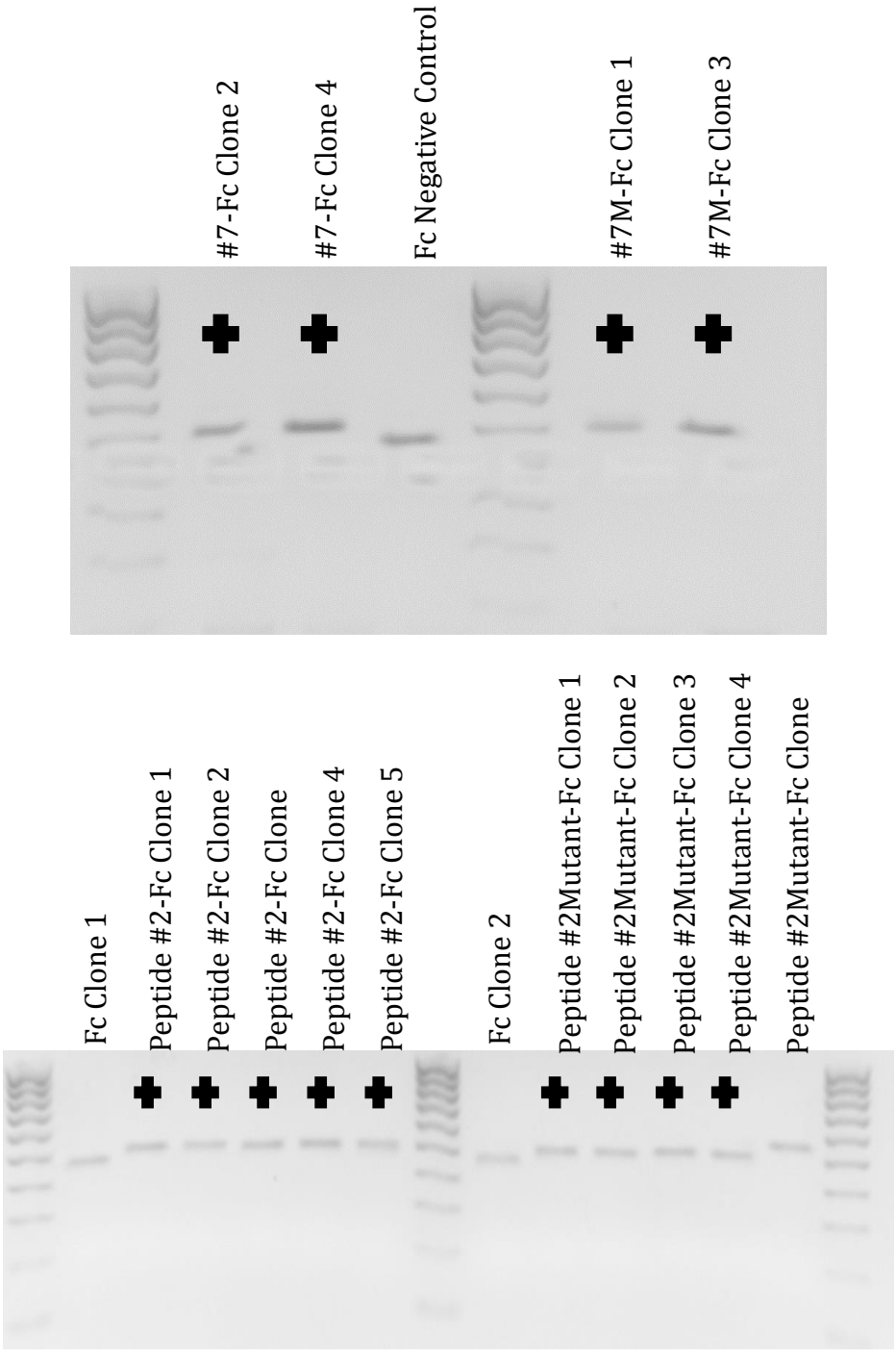

Figure 8. Digestion Gel of Fused Plasmids. Digestion gel used to confirm uptake of peptide coding sequence into mIgG2a Fc2 plasmid, untreated plasmid used as negative control.

4.2 Expression and secretion of Fc fusion proteins

Fusion plasmids were transfected with FuGene6 as optimized at a 3:1 ratio with DNA into CHO-K1 cells at a density of $2x10^5$. Cells and supernatants were harvested 48 hours later. Western blots were then performed to confirm expression and secretion in cell lysate and supernatants respectively (figure 9a). Protein productivity was quantitated by ELISA for the mouse immunoglobulin G2a from cell supernatants as well (figure 9b).

All fusion proteins were confirmed for expression and secretion by western blot and in quantifiable amounts by ELISA. However, mutated peptide fusion proteins, Peptide #7Mutant-Fc and Peptide #2Mutant-Fc, were secreted in higher amounts than their counterparts. Peptide #7-Fc gave conflicting observations, showing very low amounts of protein signal in cell supernatant by western blot and very high levels of protein by ELISA. This observation was confirmed in multiple transfections in CHO-K1 cells and replicated in human embryonic kidney 293T (HEK293T) cells (figure 10). This led us to focus all further work on Peptide #2-Fc.

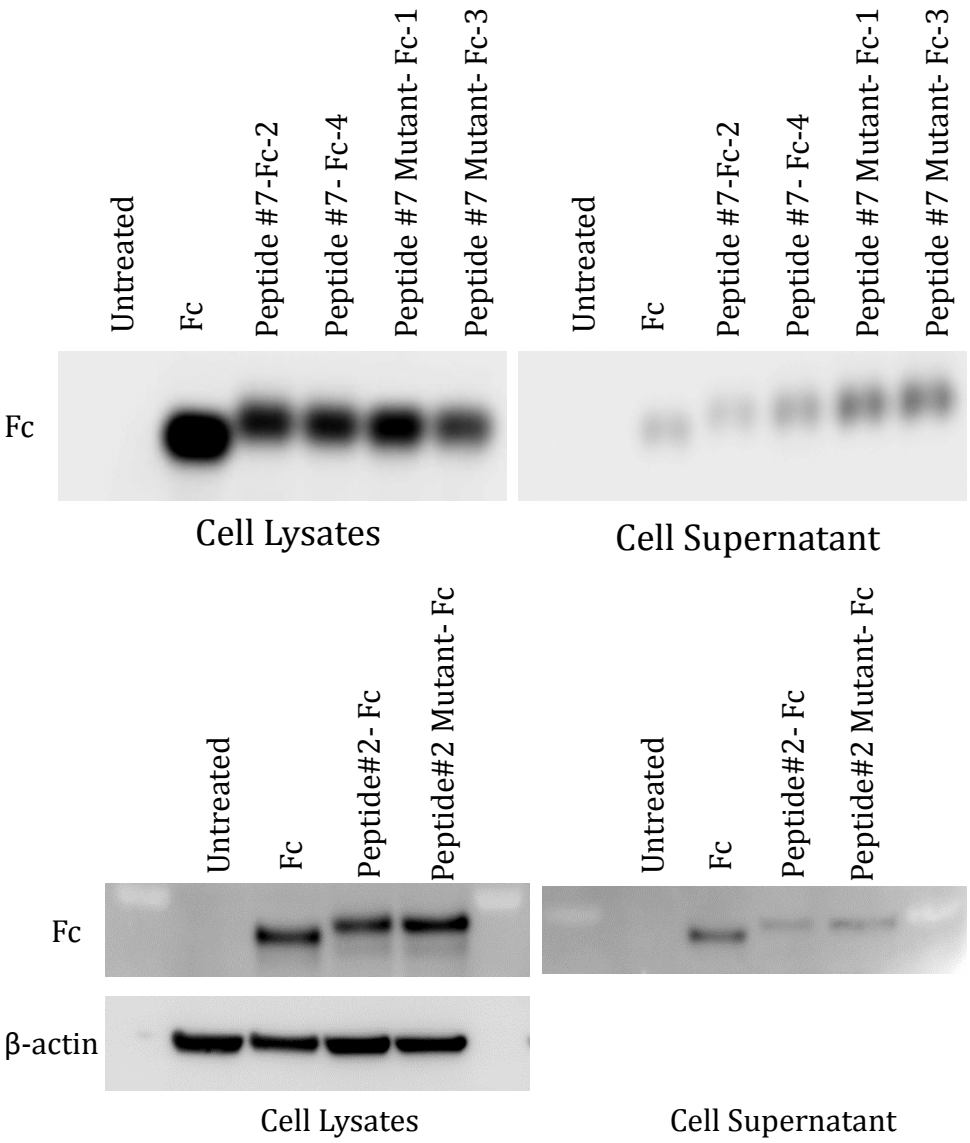

Figure 9a. Fc Fusion Protein Expression in CHO-K1 Cells. 30µg protein, as measured by Bradford assay, loaded per lane for Peptide #7 constructs. 20µL ProteoJET lysed cells from Peptide #2 constructs transfection loaded per lane, and confirmed equal by β-actin levels. 20µL of all supernatants were run in corresponding wells.

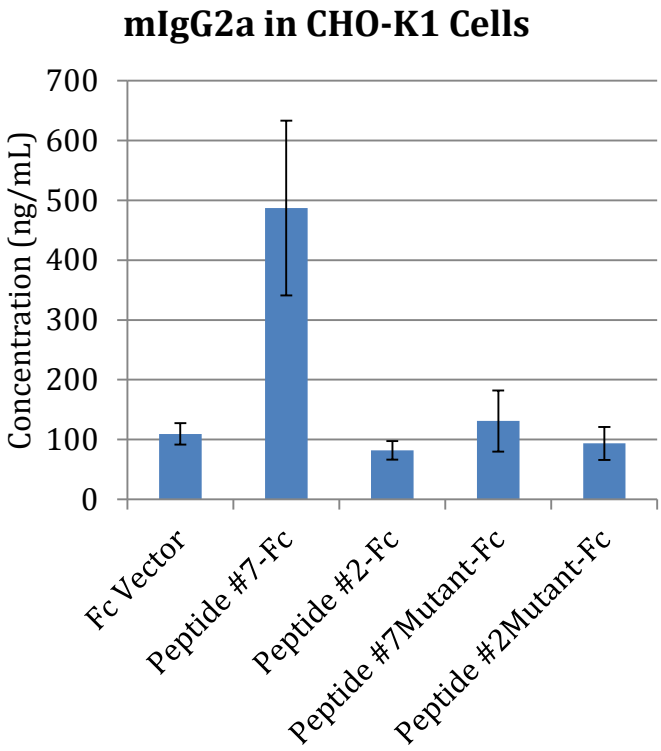

Figure 9b. Mouse IgG2a ELISA Used to Quantitate Protein Secretion. mIgG2a ELISA kit from eBioscience used to quantify the amount of fusion protein secreted from transfected CHO-K1 cells. Average of two experiments performed in duplicate.

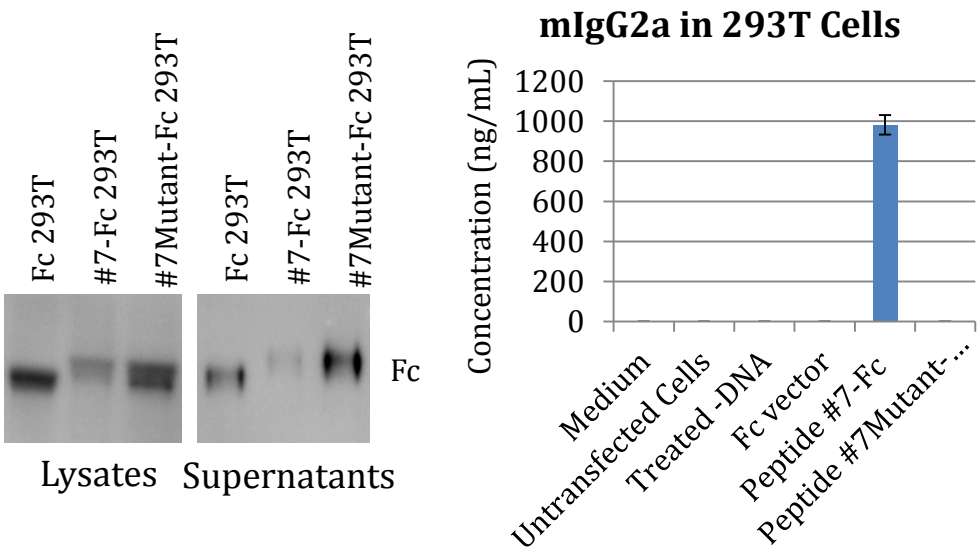

Figure 10. Transient Expression of Fusion Proteins in HEK293T cells. Similar contradictory data of western compared to ELISA seen in HEK293T cells as was previously seen in CHO-K1 cells. ELISA completed in duplicate in three different dilutions per sample.

4.2.1 Confirmation of fusion protein binding to IL-23 receptor

An immunoprecipitation was done to confirm that the mature Peptide #2-Fc could still bind to the IL-23 receptor. Cell supernatants were mixed with Protein A resin to bind the fusion protein, then resin was incubated overnight in medium containing Δ9. Δ9 is the IL-23 receptor lacking its transmembrane domain coded by exon 9 (Kan, et al. 2008). Thus it is the soluble form of the receptor with the cytokine binding region intact. Peptide #2-Fc displayed receptor binding as shown by western blot of IP products probed for the IL-23 receptor. Presence of IgG2a Fc and Peptide #2Mutant-Fc proteins were confirmed by the presence of the Fc protein, but did not show IL-23 receptor binding (figure 11).

4.2.2 Generation and validation of stable cell lines

In order to generate protein in a more efficient manner, peptide-Fc fusion plasmids were transfected into CHO-K1 cells and selected for using Zeocin™ at 250μg/mL for two weeks. Cells were then plated at $2x10^5$ cells per well of 6-well plates to be compared alongside transient transfected cells. After 48 hours, cell supernatants were harvested and quantitated for protein productivity by mouse IgG2a ELISA (figure 12). The two highest producing clones were kept growing for protein collection: clones 1 and 4 for Peptide #2-Fc and clones 1 and 5 for Peptide #2Mutant-Fc. All others were frozen down.

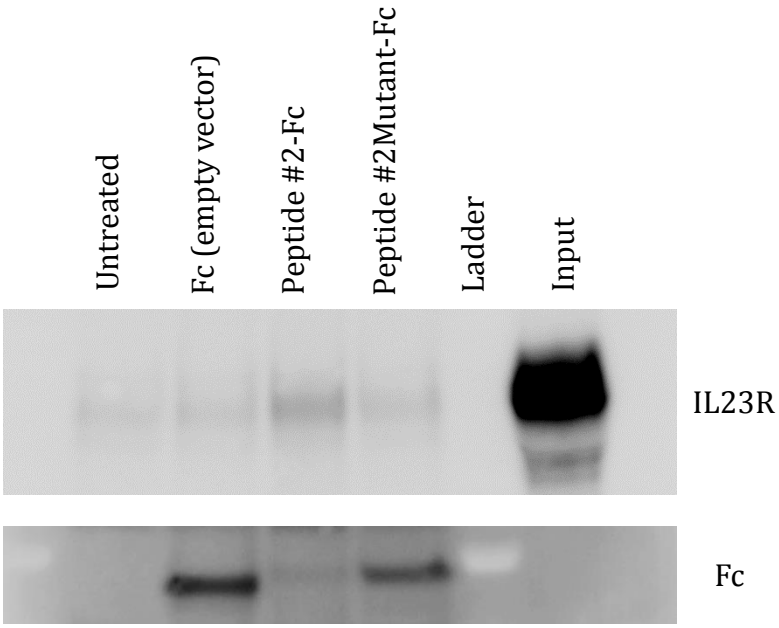

Figure 11. In Vitro Binding Assay. Used IL-23R Δ9 in immunoprecipitation with fusion proteins to show binding of Peptide #2-Fc to the IL-23R and not the mutated peptide or the Fc portion of the protein.

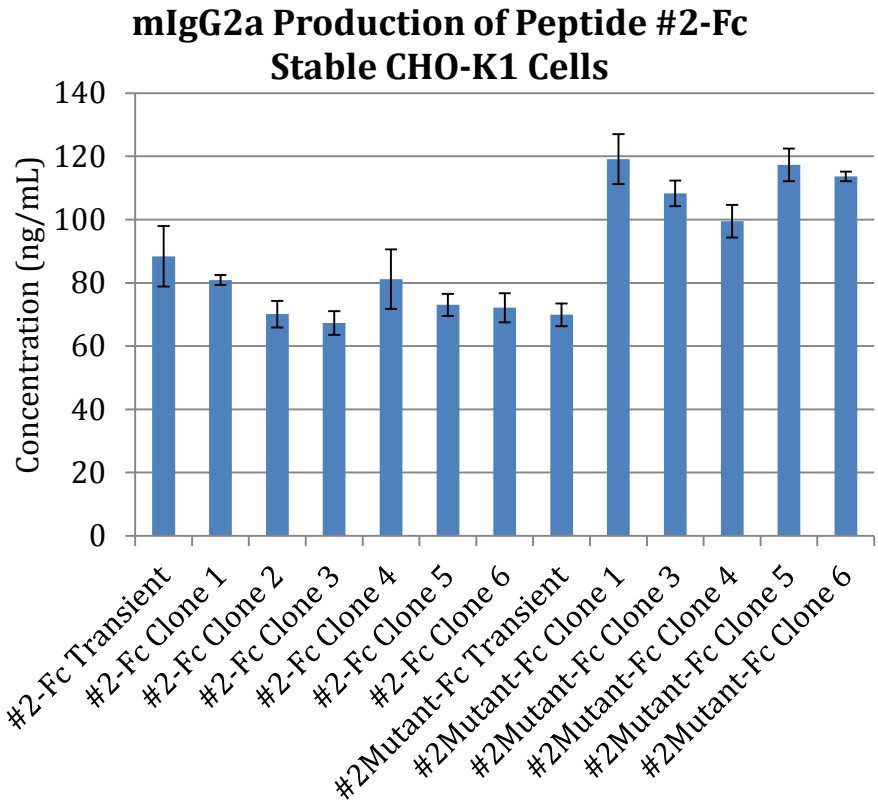

Figure 12. Mouse IgG2a ELISA Was Used to Measure Protein Productivity of CHO-K1 Derived Stable Cell Lines. One experiment was performed in duplicate and compared to cell supernatant of transiently expressing cells.

4.3 Protein purification

Peptide #2-Fc and Peptide #2Mutant-Fc proteins were purified on a Protein A column from serum free cell supernatant of stable cell lines. After several collections, pure protein samples in 1x PBS were run on an SDS-PAGE gel and stained with Coomassie Blue to check protein purity (figure 13a). The left most sample of each protein had been purified on an Ultra Protein A column. The phenomenon cannot be explained, but subsequent samples were purified using Ultra Protein A. Unclean protein was combined and also run through an Ultra Protein A column, after which they were found clear of any contamination.

When the purification protocol was first being tested, all column flow through and the first half of the washes were collected for testing of presence of fusion protein product. They were assessed by western blot alongside column eluents of fusion protein and cell supernatants were used as a positive control. Figure 13b is an example of just one of these blots, depicting no protein loss for Peptide #2Mutant-Fc, but all others looked the same. This confirmed the Protein A column purification protocol we designed to collect all fusion protein products without significant losses.

4.3.1 Fusion protein binding to IL-23 receptor

Immunoprecipitation with Δ9 was repeated with 5μg pure protein to rule out any other possible artifacts seen previously (figure 14).

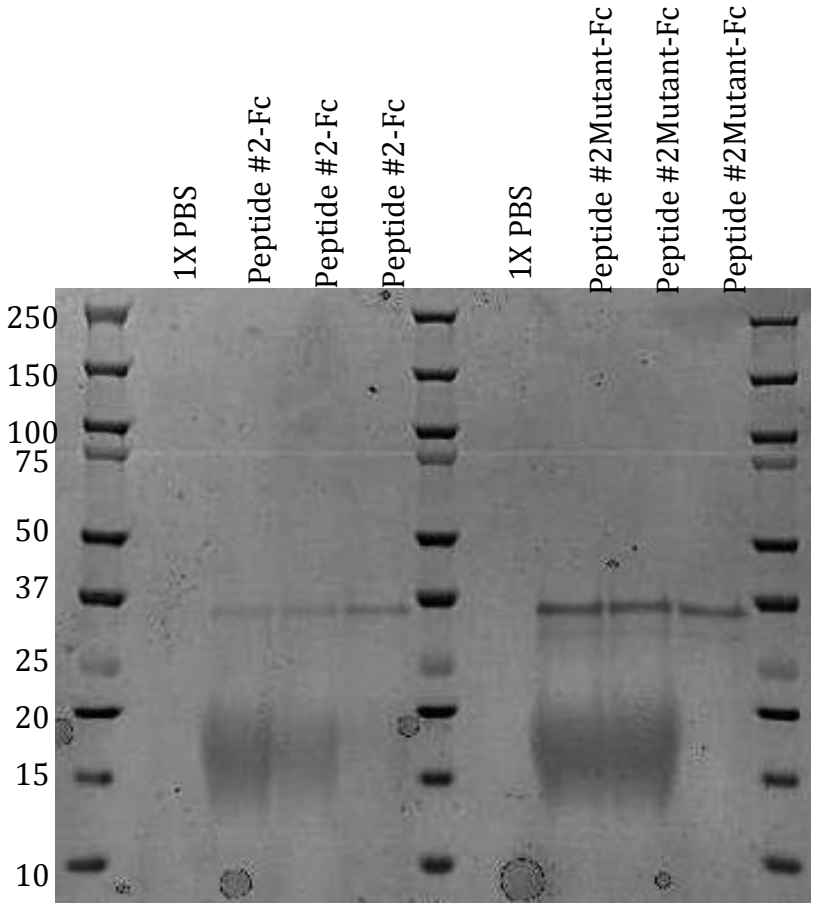

Figure 13a. Purity of Collected Fusion Proteins by Coomassie Blue Staining. 1X PBS was used as negative control since it is the background buffer for the fusion proteins. First two collections were purified using GenScript Protein A resin and gave the unknown artifact seen at approximately 17kDa, while the third collection was purified by GenScript Ultra Protein A resin and this band was not observed.

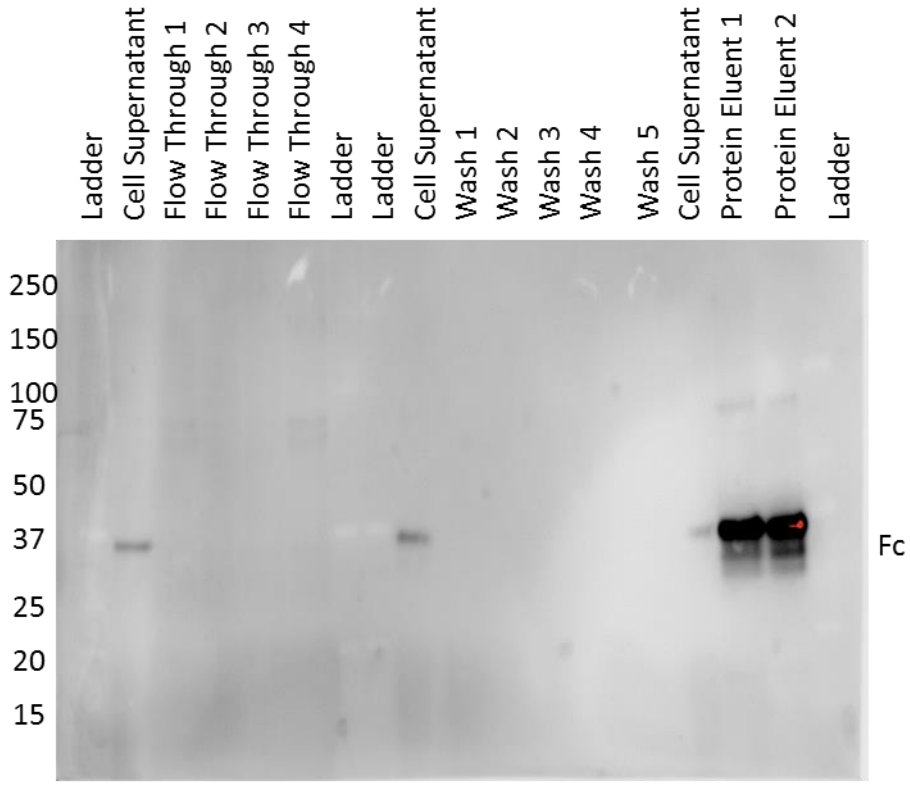

Figure 13b. Western Blot of Protein Purification Steps.
Collected all flow throughs from column and first five washes to determine efficiency of column purification.

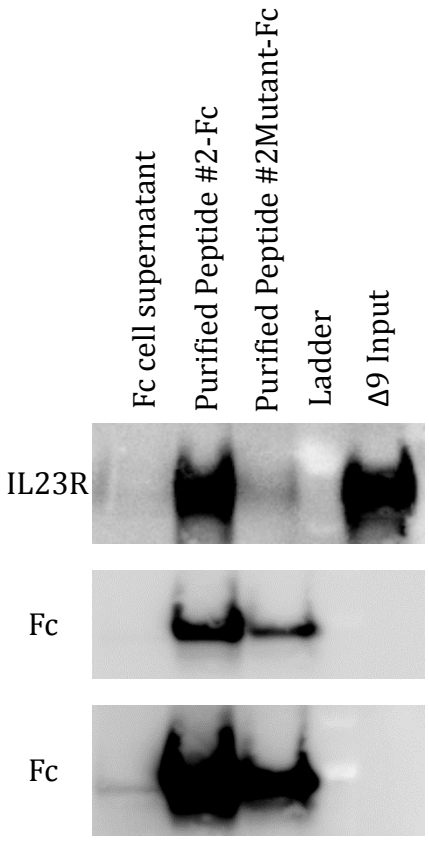

Figure 14. Immunoprecipitation of Fusion Proteins with Δ9. IgG2a Fc transfect CHO-K1 cell supernatant and Peptide #2Mutant-Fc were used and negative controls for IL-23 receptor binding. α-mouse IgG-Fc fragment was used as a control to confirm protein presence, which was exposed for 2 seconds in the middle panel and 30 second in the bottom panel to confirm presence of unmodified Fc protein.

4.4 IC_{50} determination in cell-free ELISA

In order to determine the IC_{50} value for the fusion proteins, a cell-free competitive ELISA was utilized. When testing an inhibitor, the natural ligand, or IL-23 in this case, is held constant in the linear range of stimulation curve while the inhibitor is titrated in different concentrations. Typically, the half maximal effective concentration (EC_{50}) or EC75, 75% of maximal, of the ligand is used for this purpose. To this end, a dose response curve of IL-23 on the IL-23Rα was generated to establish the EC_{50} and EC_{75} concentrations (figure 15). The EC_{75} was approximately 15.625ng/mL and was thus chosen for competition with the peptide inhibitors.

To assess the value of the Peptide #2-Fc, the IC_{50} for free linear Peptide #2 was elucidated at 17.64nM (figure 16). The IC_{50} calculations for the Fc fusion proteins were complicated by the dimerization of the Fc fusion proteins. Fc fusion proteins are known to dimerize, similar to their natural antibody counterpart, but whether or not both peptides of a dimer are sterically able to bind to the IL-23 receptor is unknown. Therefore, we have calculated the IC_{50} values considering both avenues. Assuming that only one peptide of a dimer can bind at a time, Peptide #2-Fc gave an IC_{50} of 239.696nM, which is a 14-fold increase over the independent Peptide #2, and if both are active, the IC_{50} is 479.393nM or a 27-fold increase over Peptide #2 (figure 17). Our control, Peptide #2Mutant-Fc gave an IC_{50} values of 0.1683pM and 0.4391pM for single and dual peptide activity respectively. When looked at more closely, the line that Peptide #2Mutant-Fc produced is

not a curve at all, practically a straight line. Of additional note, the Hill slope, which is derived from the law of mass action, provides information as to whether a single enzyme is being inhibited. Inhibitors that bind to a single binding site on the enzyme should yield concentration response curves with a Hill slope of 1.0 (Scott and Williams, 2012). Since the Hill slope for Peptide #2Mutant-Fc is -2.744 by Best-fit calculations and undefined for the 95% confidence interval, we can assume that this fusion protein is not an effective inhibitor as initially anticipated.

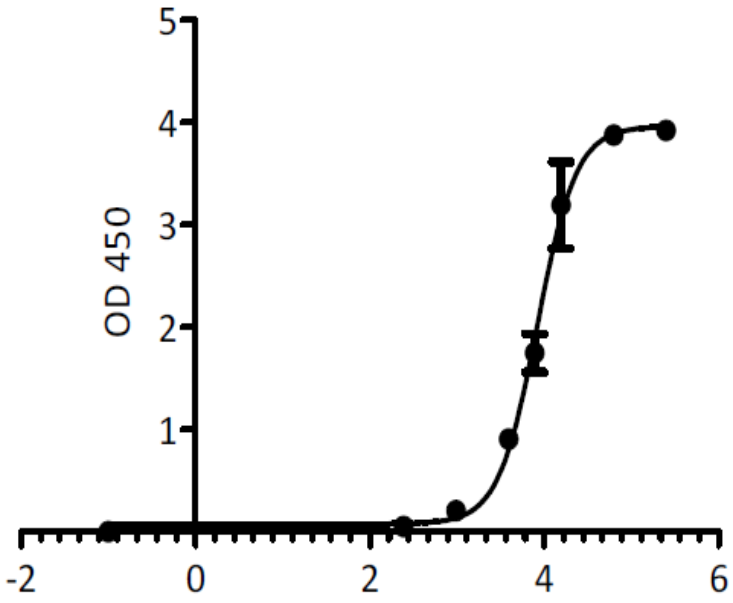

	EC_{50}	Hill Slope
Best-fit Value	8.338ng/mL	1.949
95% Confidence Interval	7.046- 9.866ng/mL	1.344-2.554

Figure 15. Standard Curve of IL-23 in IL-23 Receptor Competitive ELISA. Used to determine linear region of curve to hold IL-23 concentration at for competition with peptide. Experiment conducted three times in duplicate.

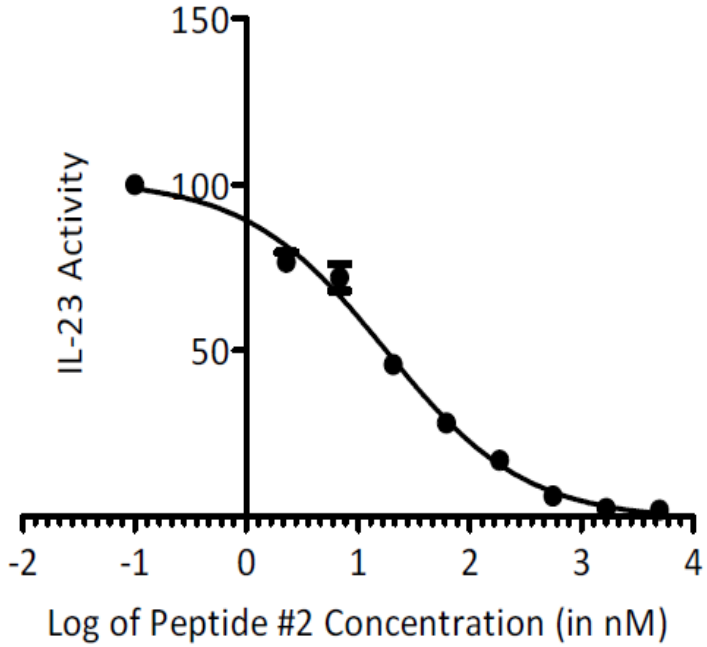

	IC_{50}	Hill Slope
Best-fit Value	17.64nM	-0.6944
95% Confidence Interval	13.26-23.46nM	-0.8303-(-)0.5585

Figure 16. Dosage Curve of Peptide #2 in IL-23 Receptor Competitive ELISA. Started at 5μM with 3-fold dilution. Average of three experiments completed in duplicate shown.

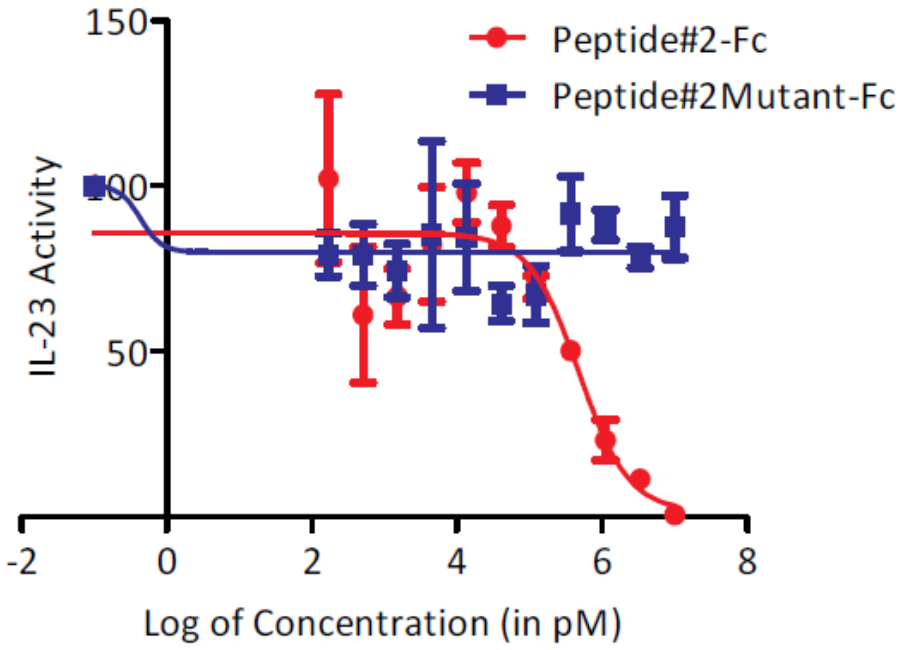

Dual Calculation

	Peptide #2-Fc IC_{50}	Peptide #2 Mutant -Fc IC_{50}
Best-fit Value	479.393nM (-1.275)	~ 0.4391 pM (~ -2.969)
95% Confidence Interval	161.074-1427nM (-2.771-0.2207)	Very wide

Sinlge Calculation

	Peptide #2-Fc IC_{50}	Peptide #2 Mutant -Fc IC_{50}
Best-fit Value	239.696nM (-1.275)	~ 0.1683 pM (~ -2.744)
95% Confidence Interval	80.537-71.3390nM (-2.771-0.2207)	Very wide

Figure 17. Dosage Curve of Fc-Fusion Proteins in IL-23 Receptor Competitive ELISA. Peptide #2-Fc is shown in red and Peptide #2 Mutant-Fc is in blue. Calculations below are completed for both scenarios as if only one peptide of the dimerized fusion protein is active or both peptides are active. Hill slopes are shown in parentheses. Average of two experiments in duplicate.

4.5 IC_{50} determination in cell-based STAT3-luciferase reporter assay

Whereas the cell-free ELISA examined Peptide #2-Fc binding to the IL23Rα specifically, the cell-based STAT3-Luciferase reporter assay investigated the fusion protein's ability to inhibit cytokine binding to a complete IL-23 receptor with both IL12Rβ1 and IL23Rα chains present. This assay also considered the implications downstream of receptor binding. For although it was known that Peptide #2-Fc effectively bound to the IL23Rα chain and inhibited p19 of the IL-23 cytokine from binding, it was not known whether this actually inhibited whether or not Peptide #2 was still able to inhibit the subsequent phosphorylation of STAT3 when fused to the Fc protein.

Similarly to the cell-free ELISA, a standard curve with IL-23 was tested to determine the EC_{50} in this assay. When an 8-point 3-fold dilution standard curve starting at 300ng/mL proved appeared to be on the cusp of plateau, two higher points were added (figure 18). However, the dose curve still did not reach maximal. Experiments with IL-23 added from stock concentration, or 4545ng/mL, in an 8-point 4-fold dilution curve were attempted, but they resulted in stimulation curves with Hill slopes of 0.1 to 0.5. Scott and Williams suggests that a Hill slope of this magnitude is possibly due to more than one enzyme contributing to the overall signal, which probable considering this assay senses STAT3 phosphorylation. Thus, we decided to use IL-23 at 25ng/mL as the competing concentration in this assay, because it

fell in the linear range of stimulation, which is enough to then compare the IC_{50} values among the peptide unknowns.

Unmodified Peptide #2 yielded an IC_{50} value of 4.807μM with a 95% confidence interval of 3.719-6.211μM (figure 19). Again, calculations for single versus dual activity of Peptide #2 in the Fc dimer were made from the dose-dependent curve from two experiments performed in duplicate (figure 20). Assuming single Peptide #2 activity in the Fc dimer, we observe an IC_{50} of 0.8105μM or a 6-fold decrease over Peptide #2. If both peptides on the Fc dimer are active, the IC_{50} value becomes 1.621μM, which is only a 3-fold decrease. Since we are considering an inhibitor, this is an even better result than expected, considering the data generated by the competitive ELISA. This observation leads to the hypothesis that something is limiting the in the ELISA, either due to steric availability or limiting by the two dimensional space as opposed to the three dimensional environment of the cell-based assay. Similar to the ELISA assay, Peptide #2Mutant-Fc also suggested an IC_{50} value of single acting at 2.993μM or 5.987μM for dual activity, but as previously seen, the Hill slope is of high magnitude, indicating that is inhibiting non-specifically (Scott and Williams, 2012).

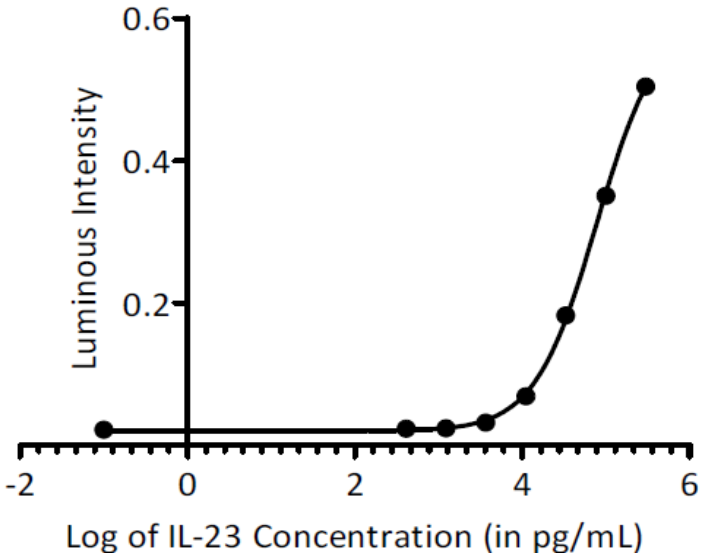

	EC_{50}	Hill Slope
Best-fit Value	77.232ng/mL	1.181
95% Confidence Interval	65.179-91.513ng/mL	1.034-1.327

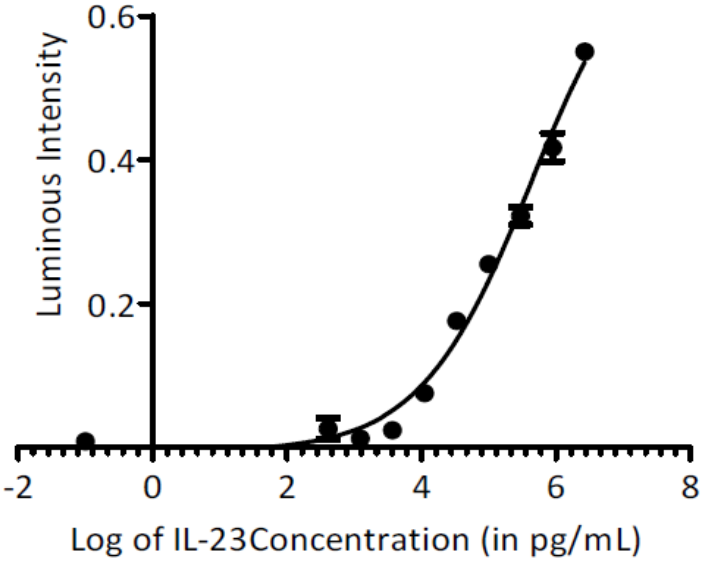

	EC_{50}	Hill Slope
Best-fit Value	424.532/mL	0.5256
95% Confidence Interval	171.105-1053ng/mL	0.4016-0.6496

Figure 18. Standard Curve of IL-23 in STAT3-Luciferase Assay. Used to determine linear region of curve to hold IL-23 concentration at for competition with peptide. Top panel is 3-fold dilution from 300ng/mL completed twice in sextets each. The same was done on the lower panel, adding two points at the top of the curve to start at 2700ng/mL.

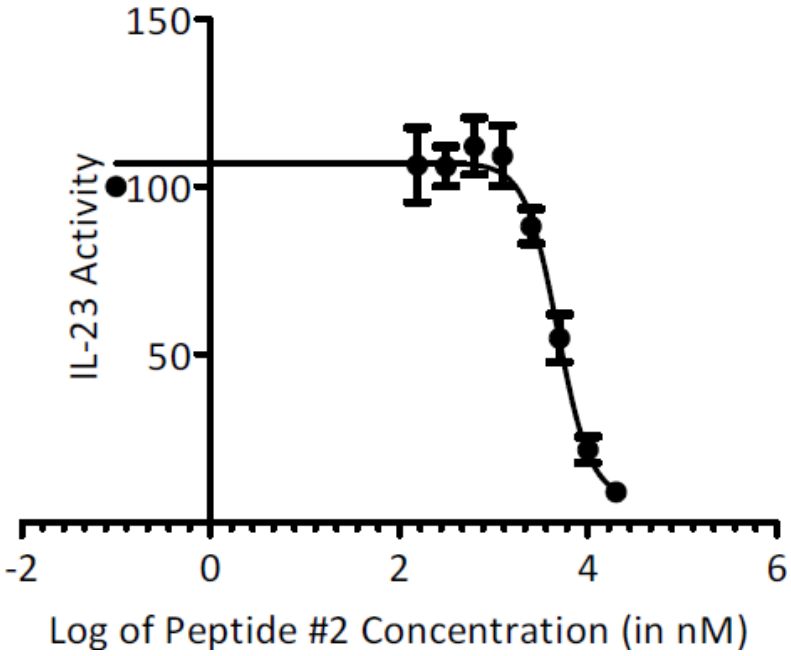

	IC_{50}	Hill Slope
Best-fit Value	4.807μM	-2.513
95% Confidence Interval	3.719-6.211μM	-3.924-(-)1.103

Figure 19. Dosage Curve of Peptide #2 in STAT3-Luciferase Assay. Started at 20μM with 2-fold dilution. Average of three experiments completed in duplicate shown.

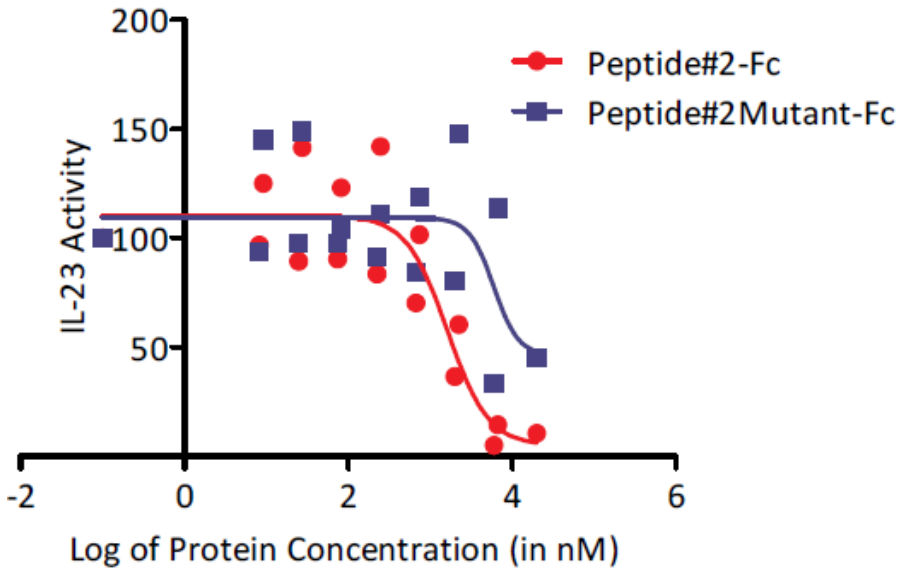

Dual Calculation

	Peptide #2-Fc IC_{50}	Peptide #2Mutant-Fc IC_{50}
Best-fit Value	1.621µM (-1.733)	5.987µM (-2.904)
95% Confidence Interval	0.6514-4.034µM (-4.022-0.5553)	1.461-24.540µM (-19.40-13.59)

Single Calculation

	Peptide #2-Fc IC_{50}	Peptide #2Mutant-Fc IC_{50}
Best-fit Value	0.8105µM (-1.733)	2.993µM (-2.904)
95% Confidence Interval	0.3257-2.017µM (-4.022-0.5553)	0.7303-12.269µM (-19.40-13.59)

Figure 20. Dosage Curve of Fc-Fusion Proteins in STAT3-Luciferase Assay. Peptide #2-Fc is shown in red and Peptide #2 Mutant-Fc is in blue. Calculations below are completed for both scenarios as if only one peptide of the dimerized fusion protein is active or both peptides are active. Hill slopes are shown in parentheses.

5. Discussion

This study has found that the fusion of the mouse IgG2a-Fc heavy chain to Peptide #2 is a viable option as a drug delivery system for this therapeutic peptide. However, the same cannot be said for Peptide #7, because experimental complications led to inconclusive data for this fusion protein. Peptide #2-Fc performs better than the unmodified Peptide #2 in our cell-based assay, and arguably overall, for Peptide #2-Fc is a much larger compound that Peptide #2 alone and therefore, probably experienced some steric constraints in the two dimensional system of the ELISA where the Peptide had none.

To truly comprehend the benefits of Peptide #2-Fc, it would be advantageous to include comparisons other therapies that target the same interaction in our assays. For instance, Centocor Ortho Biotech has launched Stelara™ (ustekinumab), a monoclonal human IgG1κ antibody that binds to the p40 molecular shared by IL-12 and IL-23 (Luo et al., 2010). It is currently indicated for treatment of plaque psoriasis in Europe, the US, and Japan (Tang et al., 2011), and is still being tested for approval for treatment of psoriatic arthritis (Gottlieb et al., 2009) and Crohn's disease (Sandborn et al., 2008). However, Ustekinumab was previously assessed for the treatment of MS and discontinued when it failed to reduce the number of lesions seen and caused serious injection site reactions compared to those receiving placebo (Segal et al., 2008). Longbrake and Ranke criticized the trial for the inclusion of patients with advanced disease, citing that the drug's efficacy may be improved if only given in the early stage of disease (Longbrake & Ranke,

2009). Other monoclonal antibodies active against p40 are also being developed by different companies, but have yet to reach the market to use for comparison.

Several companies have other drugs of interest for comparison as well, focusing on αp19 monoclonal antibodies and inhibiting IL-23 cytokine production, but they are not yet available for this purpose. Schering-Plough elucidated the crystal structure of IL-23 in complex with a neutralizing antibody (Beyer et al., 2008), and their original proof of concept study in autoimmune encephalomyelitis proved effective in blocking invasion of inflammatory cells to into the central nervous system, blocking acute disease and relapse (Chen et al., 2006). Since being taken over by Merck, the humanized IgG1 monoclonal antibody against p19, Tildrakizumab, has now moved into phase III clinical trials (Reichert, 2013). Also of interest is Synta Pharmaceuticals' small molecule, apilimod, which has shown reduce the production of IL-12 and IL-23 and dendritic cell infiltration in psoriasis in a phase IIa clinical trial (Wada et al., 2012). Yet all of the these different treatment options are all alike in that they are focusing on modification of the cytokine, whereas our own Peptide #2-Fc acts directly on the IL-23 receptor. It also specifically acts on the IL-23 receptor specifically and would, therefore, not interfere with IL-12 signaling as with the αp40 monoclonal antibodies and apilimod.

Further complicating the targeting of IL-23 is the discovery of new subsets of cells that express the IL-23 receptor. Lockhart et al. was the first to reveal a subset of γδ T cells that produced IL-17 (Lockhart et al., 2006), but

these cells requirement of IL-23 was not confirmed until later (Sutton et al., 2009). Unlike their αβ counterpart, Th17 cells, these γδ T cells do not need to be activated to express the IL-23 receptor, as shown by their production of IL-17 after stimulation with IL-1 and IL-23 without previous TLR2 activation (Sutton et al., 2009). Since γδ T cells are found on mucosal surfaces, e.g. the lining of the gut, it will be interesting to learn the full extent of their involvement in autoimmune diseases like IBD.

The IL-23 receptor has also been located on innate lymphoid cells (ILC) (Buonocore et al., 2010). Although these cells have been slowly identified and studied over the past decade, it was only recently proposed to classify them as their own group of cells and further clarify them into subsets (Spits et al., 2013). Common lymphoid progenitor cells also produce higher amounts of IL-22, IL-17, and IFNγ when exposed to IL-23 (Buonocore et al., 2010). Although, these advances may seem to be detrimental to the development of an IL-23 therapy of any kind, in fact, this new information may prove to enhance treatment options. For instance, Peptide #2-Fc could be combined with a current treatment for IBD, Nuvion (Visilizumab), which targets the cell marker CD3 found on activated T cells (Trajkovic, 2002). This would target the IL-23 receptor on a specific cell type, which may prove to be more advantageous by disease type.

Alternative delivery methods could also help direct disease specific treatment. For example, human skin has been shown to be permeable to small peptides (Dawson et al., 1990), meaning that Peptide #2 could be directly absorbed at psoriatic lesion sites to stop and hopefully reverse

formation. Oral formulations are also now possible thru formulation with PEG linked low molecular weight protamine to increase intestinal absorption (He et al., 2013). This preparation could be beneficial to IBD patients since PEG 15-20 has previously displayed protective effects in the intestines (Valuckaite et al., 2009). Nanocarriers are another highly appealing option as well as they have been proven a safe and effective oral formulation (Tankó et al., 2004). They have even been demonstrated to be able to pass through the blood-brain barrier (Caban et al., 2012), which would prove beneficial for possible MS treatments, including our very own Peptide #2.

6. Summary and Conclusions

The originally proposed Peptide #7-Fc fusion protein was able to be expressed, but not secreted in adequate amounts for protein purification, shifting the focus of this study to Peptide #2-Fc. This fusion protein was expressed and secreted in satisfactory quantities to allow for mass purification.

Purified Peptide #2-Fc was then characterized using both cell-free and cell-based assays alongside the unmodified Peptide #2. The fusion protein performed worse than Peptide #2 in the cell-free competitive ELISA with a 27-fold increase in IC_{50} value, whereas, it achieved a 3-fold lower IC_{50} value than Peptide #2 in the cell-based assay. However, in both assays the IC_{50} values for Peptide #2-Fc were practical to support further studies into this formulation for a possible drug therapy.

This study opens the door for the future utilization of Peptide #2 as a drug candidate for uses in many IL-23 related diseases, including IBD, psoriasis, and MS.

7. Bibliography

Autoimmune Diseases Coordinating Committee of the National Institutes of Health. "Progress in Autoimmune Diseases Research." Report to Congress. March 2005. Retrieved on April 4, 2013 from http://www.niaid.nih.gov.

Beyer BM, Ingram R, Ramanathan L, Reichert P, Le HV, Madison V, Orth P. Crystal structures of the pro-inflammatory cytokine interleukin-23 and its complex with a high-affinity neutralizing antibody. J Mol Biol. 2008 Oct 17;382(4):942-55. doi: 10.1016/j.jmb.2008.08.001. Epub 2008 Aug 7. PubMed PMID: 18708069.

Caban S, Capan Y, Couvreur P, Dalkara T. Preparation and characterization of biocompatible chitosan nanoparticles for targeted brain delivery of peptides. Methods Mol Biol. 2012;846:321-32. doi: 10.1007/978-1-61779-536-7_27. PubMed PMID: 22367822.

Chen Y, Langrish CL, McKenzie B, Joyce-Shaikh B, Stumhofer JS, McClanahan T, Blumenschein W, Churakovsa T, Low J, Presta L, Hunter CA, Kastelein RA, Cua DJ. Anti-IL-23 therapy inhibits multiple inflammatory pathways and ameliorates autoimmune encephalomyelitis. J Clin Invest. 2006 May;116(5):1317-26. PubMed PMID: 16670771; PubMed Central PMCID: PMC1450386.

Centers for Disease Control and Prevention. (2011 July 15) Inflammatory Bowel Disease. *Centers for Disease Control and Prevention*. Retrieved April 4, 2013 from http://www.cdc.gov.

Dawson BV, Hadley ME, Levine N, Kreutzfeld KL, Don S, Eytan T, Hruby VJ. In vitro transdermal delivery of a melanotropic peptide through human skin. J Invest Dermatol. 1990 Apr;94(4):432-5. PubMed PMID: 2155969.

Deenick EK, Tangye SG. Autoimmunity: IL-21: a new player in Th17-cell differentiation. Immunol Cell Biol. 2007 Oct;85(7):503-5. Epub 2007 Sep 4. Review. Erratum in: Immunol Cell Biol. 2008 Jul;86(5):478. PubMed PMID: 17768419.

Di Cesare A, Di Meglio P, Nestle FO. The IL-23/Th17 axis in the immunopathogenesis of psoriasis. J Invest Dermatol. 2009 Jun;129(6):1339-50. doi: 10.1038/jid.2009.59. Epub 2009 Mar 26. Review. PubMed PMID: 19322214.

Gallagher, G., Yu, R., Brazaitis, J. (2013). *US Patent No. 20,130,029,907*. Washington, DC: U.S. Patent and Trademark Office.

Gallagher, G., Yu, R., Brazaitis, J. (2013). *US Patent No. 20,130,172,272*. Washington, DC: U.S. Patent and Trademark Office.

Gottlieb A, Menter A, Mendelsohn A, Shen YK, Li S, Guzzo C, Fretzin S, Kunynetz R, Kavanaugh A. Ustekinumab, a human interleukin 12/23 monoclonal antibody, for psoriatic arthritis: randomised, double-blind, placebo-controlled, crossover trial. Lancet. 2009 Feb 21;373(9664):633-40. doi: 10.1016/S0140-6736(09)60140-9. Epub 2009 Feb 11. Erratum in: Lancet. 2010 Nov 6;376(9752):1542. Lancet. 2009 Apr 18;373(9672):1340. PubMed PMID: 19217154.

He H, Sheng J, David AE, Kwon YM, Zhang J, Huang Y, Wang J, Yang VC. The use of low molecular weight protamine chemical chimera to enhance monomeric insulin intestinal absorption. Biomaterials. 2013 Oct;34(31):7733-43. doi: 10.1016/j.biomaterials.2013.06.047. Epub 2013 Jul 14. PubMed PMID: 23863452; PubMed Central PMCID: PMC3766633.

Ivanov II, McKenzie BS, Zhou L, Tadokoro CE, Lepelley A, Lafaille JJ, Cua DJ, Littman DR. The orphan nuclear receptor RORgammat directs the differentiation program of proinflammatory IL-17+ T helper cells. Cell. 2006 Sep 22;126(6):1121-33. PubMed PMID: 16990136.

Lockhart E, Green AM, Flynn JL. IL-17 production is dominated by gammadelta T cells rather than CD4 T cells during Mycobacterium tuberculosis infection. J Immunol. 2006 Oct 1;177(7):4662-9. PubMed PMID: 16982905.

Longbrake EE, Racke MK. Why did IL-12/IL-23 antibody therapy fail in multiple sclerosis? Expert Rev Neurother. 2009 Mar;9(3):319-21. doi: 10.1586/14737175.9.3.319. Review. PubMed PMID: 19271940.

Luo J, Wu SJ, Lacy ER, Orlovsky Y, Baker A, Teplyakov A, Obmolova G, Heavner GA, Richter HT, Benson J. Structural basis for the dual recognition of IL-12 and IL-23 by ustekinumab. J Mol Biol. 2010 Oct 8;402(5):797-812. doi: 10.1016/j.jmb.2010.07.046. Epub 2010 Aug 4. PubMed PMID: 20691190.

Oppmann B, Lesley R, Blom B, Timans JC, Xu Y, Hunte B, Vega F, Yu N, Wang J, Singh K, Zonin F, Vaisberg E, Churakova T, Liu M, Gorman D, Wagner J, Zurawski S, Liu Y, Abrams JS, Moore KW, Rennick D, de Waal-Malefyt R, Hannum C, Bazan JF, Kastelein RA. Novel p19 protein engages IL-12p40 to form a cytokine, IL-23, with biological activities similar as well as distinct from IL-12. Immunity. 2000 Nov;13(5):715-25. PubMed PMID: 11114383.

Parham C, Chirica M, Timans J, Vaisberg E, Travis M, Cheung J, Pflanz S, Zhang R, Singh KP, Vega F, To W, Wagner J, O'Farrell AM, McClanahan T, Zurawski S, Hannum C, Gorman D, Rennick DM, Kastelein RA, de Waal Malefyt R, Moore KW. A receptor for the heterodimeric cytokine IL-23 is composed of IL-12Rbeta1 and a novel cytokine receptor subunit, IL-23R. J Immunol. 2002 Jun 1;168(11):5699-708. PubMed PMID: 12023369.

Peppel K, Crawford D, Beutler B. A tumor necrosis factor (TNF) receptor-IgG heavy chain chimeric protein as a bivalent antagonist of TNF activity. J Exp Med. 1991 Dec 1;174(6):1483-9. PubMed PMID: 1660525; PubMed Central PMCID: PMC2119031.

Reichert JM. Antibodies to watch in 2013: Mid-year update. MAbs. 2013 Jul-Aug;5(4):513-7. doi: 10.4161/mabs.24990. Epub 2013 May 9. PubMed PMID: 23727858.

Sandborn WJ, Feagan BG, Fedorak RN, Scherl E, Fleisher MR, Katz S, Johanns J, Blank M, Rutgeerts P; Ustekinumab Crohn's Disease Study Group. A randomized trial of Ustekinumab, a human interleukin-12/23 monoclonal antibody, in patients with moderate-to-severe Crohn's disease. Gastroenterology. 2008 Oct;135(4):1130-41. doi: 10.1053/j.gastro.2008.07.014. Epub 2008 Jul 17. PubMed PMID: 18706417.

Scott JE, Williams KP. Validating Identity, Mass Purity and Enzymatic Purity of Enzyme Preparations. 2012 May 1 [Updated 2012 Oct 1]. In: Sittampalam GS, Gal-Edd N, Arkin M, et al., editors. Assay Guidance Manual [Internet]. Bethesda (MD): Eli Lilly & Company and the National Center for Advancing Translational Sciences; 2004-2013. Available from: http://www.ncbi.nlm.nih.gov/books/NBK91995/

Segal BM, Constantinescu CS, Raychaudhuri A, Kim L, Fidelus-Gort R, Kasper LH; Ustekinumab MS Investigators. Repeated subcutaneous injections of IL12/23 p40 neutralising antibody, ustekinumab, in patients with relapsing-remitting multiple sclerosis: a phase II, double-blind, placebo-controlled, randomised, dose-ranging study. Lancet Neurol. 2008 Sep;7(9):796-804. doi: 10.1016/S1474-4422(08)70173-X. PubMed PMID: 18703004.

Spits H, Artis D, Colonna M, Diefenbach A, Di Santo JP, Eberl G, Koyasu S, Locksley RM, McKenzie AN, Mebius RE, Powrie F, Vivier E. Innate lymphoid cells--a proposal for uniform nomenclature. Nat Rev Immunol. 2013 Feb;13(2):145-9. doi: 10.1038/nri3365. Review. PubMed PMID: 23348417.

Stockinger B, Veldhoen M, Martin B. Th17 T cells: linking innate and adaptive immunity. Semin Immunol. 2007 Dec;19(6):353-61. Epub 2007 Nov 26. Review. PubMed PMID: 18023589.

Sutton CE, Lalor SJ, Sweeney CM, Brereton CF, Lavelle EC, Mills KH. Interleukin-1 and IL-23 induce innate IL-17 production from gammadelta T cells, amplifying Th17 responses and autoimmunity. Immunity. 2009 Aug 21;31(2):331-41. doi: 10.1016/j.immuni.2009.08.001. Epub 2009 Aug 13. PubMed PMID: 19682929.

Tang C, Chen S, Qian H, Huang W. Interleukin-23: as a drug target for autoimmune inflammatory diseases. Immunology. 2012 Feb;135(2):112-24. doi: 10.1111/j.1365-2567.2011.03522.x. Review. PubMed PMID: 22044352; PubMed Central PMCID: PMC3277713.

Tankó LB, Bagger YZ, Alexandersen P, Devogelaer JP, Reginster JY, Chick R, Olson M, Benmammar H, Mindeholm L, Azria M, Christiansen C. Safety and efficacy of a novel salmon calcitonin (sCT) technology-based oral formulation in healthy postmenopausal women: acute and 3-month effects on biomarkers of bone turnover. J Bone Miner Res. 2004 Sep;19(9):1531-8. Epub 2004 Jul 26. PubMed PMID: 15312255.

Trajkovic V. Nuvion. Protein Design Labs. Curr Opin Investig Drugs. 2002 Mar;3(3):411-4. PubMed PMID: 12054088.

Valuckaite V, Zaborina O, Long J, Hauer-Jensen M, Wang J, Holbrook C, Zaborin A, Drabik K, Katdare M, Mauceri H, Weichselbaum R, Firestone MA, Lee KY, Chang EB, Matthews J, Alverdy JC. Oral PEG 15-20 protects the intestine against radiation: role of lipid rafts. Am J Physiol Gastrointest Liver Physiol. 2009 Dec;297(6):G1041-52. doi: 10.1152/ajpgi.00328.2009. Epub 2009 Oct 15. PubMed PMID: 19833862; PubMed Central PMCID: PMC2850088.

Wada Y, Cardinale I, Khatcherian A, Chu J, Kantor AB, Gottlieb AB, Tatsuta N, Jacobson E, Barsoum J, Krueger JG. Apilimod inhibits the production of IL-12 and IL-23 and reduces dendritic cell infiltration in psoriasis. PLoS One. 2012;7(4):e35069. doi: 10.1371/journal.pone.0035069. Epub 2012 Apr 6. PubMed PMID: 22493730; PubMed Central PMCID: PMC3320873.

Walsh SJ, Rau LM. Autoimmune diseases: a leading cause of death among young and middle-aged women in the United States. Am J Public Health. 2000 Sep;90(9):1463-6. PubMed PMID: 10983209; PubMed Central PMCID: PMC1447637.

Yu RY, Gallagher G. A naturally occurring, soluble antagonist of human IL-23 inhibits the development and in vitro function of human Th17 cells. J Immunol. 2010 Dec 15;185(12):7302-8. doi: 10.4049/jimmunol.1002410. Epub 2010 Nov 12. PubMed PMID: 21076058.

Zhou L, Ivanov II, Spolski R, Min R, Shenderov K, Egawa T, Levy DE, Leonard WJ, Littman DR. IL-6 programs T(H)-17 cell differentiation by promoting sequential engagement of the IL-21 and IL-23 pathways. Nat Immunol. 2007 Sep;8(9):967-74. Epub 2007 Jun 20. PubMed PMID: 17581537.

8. Appendix

8.1 Abbreviations List

IL	Interleukin
STAT	Signal transducer and activator of transcription
JAK	Janus kinase
TYK	Tyrosine kinase
Ig	Immunoglobulin
mIgG2a	Murine immunoglobulin G2a
Δ9	Soluble interleukin-23 receptor with exon 9 deletion
DC	Dendritic cell
IBD	Inflammatory Bowel Disease
TNF	Tumor necrosis factor
MS	Multiple Sclerosis

9. Attributes

Figure 1: Illustration from (Deenick & Tangye, 2007)

Figure 2: Illustration from (Di Cesare, Di Meglio, & Nestle, 2009)

Figure 3: Illustration from (Czajkowsky, et al., 2012)

Figure 4: All work by Brianna L Probasco

Figure 5: All work by Brianna L Probasco

Figure 6: Diagram only provided by Dr. Raymond Yu

Figure 7: Diagram only provided by Dr. Raymond Yu

Figure 8: All work by Brianna L Probasco

Figure 9: All work by Brianna L Probasco

Figure 10: All work by Brianna L Probasco

Figure 11: All work by Brianna L Probasco

Figure 12: All work by Brianna L Probasco

Figure 13: All work by Brianna L Probasco

Figure 14: All work by Brianna L Probasco

Figure 15: All work by Brianna L Probasco

Figure 16: All work by Brianna L Probasco

Figure 17: All work by Brianna L Probasco

Figure 18: All work by Brianna L Probasco

Figure 19: All work by Brianna L Probasco

Figure 20: All work by Brianna L Probasco